measured using BAS 2500 and Image Gauge software (Fuji Photo Film Co. Ltd.). The expression of BiP mRNA was normalized to that of β-actin. RT-PCR analysis was performed with the following primers: 5′-acctcaaacgccttctcatc-3′ and 5′-tttctgg gcaggagcagctt-3′ for SP-C, and 5′-atggggtgaggccggtgctg-3′ and 5′-cttgatgtcatcata cttgg-3′ for GAPDH.

Whole-mount *in situ* hybridization. Whole-mount *in situ* hybridization was performed using digoxigenin-labeled riboprobes as described[40] with rat BiP cDNA.

Transfection. A cDNA encoding mouse SP-C was obtained from wild-type lung mRNA using the following primers: 5′-ccttacaaaatggacatgag-3′ and 5′-cggatccacga tatagtagagtggtagct-3′. The cDNA was subcloned into a pcDNA3.1 myc-His vector (Invitrogen). The DNA sequence was verified using the Applied Biosystems ABI Prism 310 genetic analyzer. Transfection was performed with Fugene 6 (Roche).

Histochemistry. Lungs were isolated and fixed in 4% paraformaldehyde for 24 h. After fixation, they were dehydrated in increasing concentrations of ethanol and embedded in paraffin wax. Sections (8 m) were stained with hematoxylin and eosin. For immunohistochemistry, sections were incubated with 10% normal goat or bovine serum in phosphate-buffered saline (PBS) for 30 min to block non-specific antibody binding, and then incubated with a primary antibody in PBS for 12 h at 4 °C. Sections were rinsed with PBS, incubated with a secondary antibody in PBS for 2 h at room temperature and then visualized using the VECTASTAIN Elite ABC kit (Vector Laboratories) with diaminobenzidine (Sigma).

Confocal and immunofluorescence microscopy. Cells on coverslips were fixed in 2% formaldehyde in PBS for 10 min at room temperature and then processed as described.[6] Labeled cells were examined using a confocal laser scanning microscope (Axiovert 100M, LSM510, Ver. 3.2, Carl Zeiss) fitted with krypton and argon lasers and a Plan-Apochromat 100 NA 1.40 oil immersion objective.

Electron microscopy. Fifteen newborn animals and 24 embryos were processed for electron microscopy. Newborn animals were fixed within 2 h of birth. Embryos were fixed on E18.5. Before fixation, a tail sample was collected for genotyping.

Animals were anesthetized on ice. The thorax was opened, and the heart was removed with part of the large vessels. The trachea was clamped with tweezers, and both the left and right lobes of the lung were excised after cutting the trachea just proximal to the clamped site. The lung was immediately placed in a syringe filled with 3% glutaraldehyde in 10 mM HEPES, 145 mM NaCl (pH 7.4). After the air in the lung and air ducts was expelled by manipulating the plunger, the lung was cut into small pieces with a razor blade and was further fixed in the same fixative for an additional 2 h. After postfixation with 1% osmium tetroxide, the tissue was dehydrated in absolute ethanol and embedded in Epon mixture (TAAB, Berks, England). Ultra-thin sections, double-stained with uranyl acetate and lead citrate, were observed using an electron microscope (1200EX-II, JEOL, Tokyo, Japan).

Statistical analysis. Statistical analyses were performed by one-way analysis of variance and the Bonferroni test and *t*-test using KaleidaGraph software (Synergy Software, Reading, PA, USA).

Acknowledgements. We thank Dr. T Nishino for critical comments. We also thank R Kimura and R Fujii for excellent technical assistance. This work was supported by Grants-in-Aid for Science Research from the Ministry of Education, Culture, Sports, Science and Technology to TA.

1. Ellgaard L, Helenius A. Quality control in the endoplasmic reticulum. *Nat Rev Mol Cell Biol* 2003; 4: 181–191.
2. Patil C, Walter P. Intracellular signaling from the endoplasmic reticulum to the nucleus: the unfolded protein response in yeast and mammals. *Curr Opin Cell Biol* 2001; 13: 349–355.
3. Schroder M, Kaufman RJ. The Mammalian unfolded protein response. *Annu Rev Biochem* 2005; 74: 739–789.
4. Kopito RR, Ron D. Conformational disease. *Nat Cell Biol* 2000; 2: E207–E209.
5. Kaufman RJ. Orchestrating the unfolded protein response in health and disease. *J Clin Invest* 2002; 110: 1389–1398.
6. Hamada H, Suzuki M, Yuasa S, Mimura N, Shinozuka N, Takada Y *et al.* Dilated cardiomyopathy caused by aberrant endoplasmic reticulum quality control in mutant KDEL receptor transgenic mice. *Mol Cell Biol* 2004; 24: 8007–8017.
7. Oyadomari S, Koizumi A, Takeda K, Gotoh T, Akira S, Araki E *et al.* Targeted disruption of the Chop gene delays endoplasmic reticulum stress-mediated diabetes. *J Clin Invest* 2002; 109: 525–532.
8. Clark H, Clark LS. The genetics of neonatal respiratory disease. *Semin Fetal Neonatal Med* 2005; 10: 271–282.
9. Korimilli A, Gonzales LW, Guttentag SH. Intracellular localization of processing events in human surfactant protein B biosynthesis. *J Biol Chem* 2000; 275: 8672–8679.
10. Mulugeta S, Nguyen V, Russo SJ, Muniswamy M, Beers MF. A surfactant protein C precursor protein BRICHOS domain mutation causes endoplasmic reticulum stress, proteasome dysfunction, and caspase 3 activation. *Am J Respir Cell Mol Biol* 2005; 32: 521–530.
11. Bridges JP, Xu Y, Na CL, Wong HR, Weaver TE. Adaptation and increased susceptibility to infection associated with constitutive expression of misfolded SP-C. *J Cell Biol* 2006; 172: 395–407.
12. Beers MF, Mulugeta S. Surfactant protein C biosynthesis and its emerging role in conformational lung disease. *Annu Rev Physiol* 2005; 67: 663–696.
13. Hendershot LM. The ER function BiP is a master regulator of ER function. *Mt Sinai J Med* 2004; 71: 289–297.
14. Sonnichsen B, Fullekrug J, Nguyen Van P, Diekmann W, Robinson DG, Mieskes G. Retention and retrieval: both mechanisms cooperate to maintain calreticulin in the endoplasmic reticulum. *J Cell Sci* 1994; 107: 2705–2717.
15. Bertolotti A, Zhang Y, Hendershot LM, Harding HP, Ron D. Dynamic interaction of BiP and ER stress transducers in the unfolded- protein response. *Nat Cell Biol* 2000; 2: 326–332.
16. Hammond C, Helenius A. Quality control in the secretory pathway: retention of a misfolded viral membrane glycoprotein involves cycling between the ER, intermediate compartment, and Golgi apparatus. *J Cell Biol* 1994; 126: 41–52.
17. Yamamoto K, Fujii R, Toyofuku Y, Saito T, Koseki H, Hsu VW *et al.* The KDEL receptor mediates a retrieval mechanism that contributes to quality control at the endoplasmic reticulum. *EMBO J* 2001; 20: 3082–3091.
18. Munro S, Pelham HR. A C-terminal signal prevents secretion of luminal ER proteins. *Cell* 1987; 48: 899–907.
19. Lewis MJ, Pelham HR. A human homologue of the yeast HDEL receptor. *Nature* 1990; 348: 162–163.
20. Beh CT, Rose MD. Two redundant systems maintain levels of resident proteins within the yeast endoplasmic reticulum. *Proc Natl Acad Sci USA* 1995; 92: 9820–9823.
21. Luo S, Mao C, Lee B, Lee AS. GRP78/BiP is required for cell proliferation and protecting the inner cell mass from apoptosis during early mouse embryonic development. *Mol Cell Biol* 2006; 26: 5688–5697.
22. Zinszner H, Kuroda M, Wang X, Batchvarova N, Lightfoot RT, Remotti H *et al.* CHOP is implicated in programmed cell death in response to impaired function of the endoplasmic reticulum. *Genes Dev* 1998; 12: 982–995.
23. Taxis C, Vogel F, Wolf DH. ER-golgi traffic is a prerequisite for efficient ER degradation. *Mol Biol Cell* 2002; 13: 1806–1818.
24. Hallman M. Lung surfactant, respiratory failure, and genes. *N Engl J Med* 2004; 350: 1278–1280.
25. Nogee LM, de Mello DE, Dehner LP, Colten HR. Brief report: deficiency of pulmonary surfactant protein B in congenital alveolar proteinosis. *N Engl J Med* 1993; 328: 406–410.
26. Clark JC, Wert SE, Bachurski CJ, Stahlman MT, Stripp BR, Weaver TE *et al.* Targeted disruption of the surfactant protein B gene disrupts surfactant homeostasis, causing respiratory failure in newborn mice. *Proc Natl Acad Sci USA* 1995; 92: 7794–7798.
27. Lahti M, Marttila R, Hallman M. Surfactant protein C gene variation in the Finnish population – association with perinatal respiratory disease. *Eur J Hum Genet* 2004; 12: 312–320.
28. Danlois F, Zaltash S, Johansson J, Robertson B, Haagsman HP, van Eijk M *et al.* Very low surfactant protein C contents in newborn Belgian White and Blue calves with respiratory distress syndrome. *Biochem J* 2000; 351 (Part 3): 779–787.
29. Kim SH, Creemers JW, Chu S, Thinakaran G, Sisodia SS. Proteolytic processing of familial British dementia-associated BRI variants: evidence for enhanced intracellular accumulation of amyloidogenic peptides. *J Biol Chem* 2002; 277: 1872–1877.
30. Nagai N, Hosokawa M, Itohara S, Adachi E, Matsushita T, Hosokawa N *et al.* Embryonic lethality of molecular chaperone hsp47 knockout mice is associated with defects in collagen biosynthesis. *J Cell Biol* 2000; 150: 1499–1506.
31. Mesaeli N, Nakamura K, Zvaritch E, Dickie P, Dziak E, Krause KH *et al.* Calreticulin is essential for cardiac development. *J Cell Biol* 1999; 144: 857–868.
32. Denzel A, Molinari M, Trigueros C, Martin JE, Velmurgan S, Brown S *et al.* Early postnatal death and motor disorders in mice congenitally deficient in calnexin expression. *Mol Cell Biol* 2002; 22: 7398–7404.
33. Zhang K, Shen X, Wu J, Sakaki K, Saunders T, Rutkowski DT. Endoplasmic reticulum stress activates cleavage of CREBH to induce a systemic inflammatory response. *Cell* 2006; 124: 587–599.
34. Wu J, Kaufman RJ. From acute ER stress to physiological roles of the unfolded protein response. *Cell Death Differ* 2006; 13: 374–384.

35. Scheuner D, Song B, McEwen E, Liu C, Laybutt R, Gillespie P. Translational control is required for the unfolded protein response and *in vivo* glucose homeostasis. *Mol Cell* 2001; 7: 1165–1176.
36. Reimold AM, Iwakoshi NN, Manis J, Vallabhajosyula P, Szomolanyi-Tsuda E, Gravallese EM. Plasma cell differentiation requires the transcription factor XBP-1. *Nature* 2001; **412**: 300–307.
37. Reimold AM, Etkin A, Clauss I, Perkins A, Friend DS, Zhang J. An essential role in liver development for transcription factor XBP-1. *Genes Dev* 2000; **14**: 152–157.
38. Haas IG. and Meo T cDNA cloning of the immunoglobulin heavy chain binding protein. *Proc Natl Acad Sci USA* 1988; **85**: 2250–2254.
39. Nagy A, Rossant J, Nagy R, Abramow-Newerly W, Roder JC. Derivation of completely cell culture-derived mice from early-passage embryonic stem cells. *Proc Natl Acad Sci USA* 1993; **90**: 8424–8428.
40. Wilkinson DG, Nieto MA. Detection of messenger RNA by *in situ* hybridization to tissue sections and whole mounts. *Methods Enzymol* 1993; **225**: 361–373.

International Journal of
HEMATOLOGY

Letter to the Editor

Unique Composition of Polycomb Repressive Complex 1 in Hematopoietic Stem Cells

Yuko Kato,[a,b] Haruhiko Koseki,[c] Miguel Vidal,[d] Hiromitsu Nakauchi,[b] Atsushi Iwama[a]

[a]Department of Cellular and Molecular Medicine, Graduate School of Medicine, Chiba University, Chiba, Japan; [b]Laboratory of Stem Cell Therapy, Center for Experimental Medicine, Institute of Medical Sciences, University of Tokyo, Tokyo, Japan; [c]RIKEN Research Center for Allergy and Immunology, Laboratory for Developmental Genetics, Yokohama, Japan; [d]Department of Developmental and Cell Biology, Centro de Investigaciones Biologicas, CSIC, Madrid, Spain

Received December 19, 2006; accepted December 28, 2006

Int J Hematol. 2007;85:179-181. doi: 10.1532/IJH97.06235

The cellular memory in chromatin modifications can be faithfully maintained through cell divisions by the counteraction of transcriptional activators of the trithorax group (TrxG) and repressors of the polycomb group (PcG) [1]. PcG proteins form multiprotein complexes that play a role in the silencing of cell type–specific target genes. At least 3 major PcG complexes have been characterized. Polycomb repressive complex 1 (PRC1) includes Bmi1/Pgcf4, Rnf110/Mel18, Phc1/Mph1/Rae28, Cbx2/M33, Scmh1, and Ring1a/b; PRC2/3 includes Eed, Enx1/Ezh2, and Suz12. The PRC1 and PRC2/3 complexes possess H2A-K119 ubiquitin E3 ligase activity and H3-K27 methyltransferase activity, respectively. Both histone modifications contribute to polycomb gene silencing. Although no physical associations between these 2 complexes have been demonstrated, H3-K27 trimethylation (H3K27me3) sites serve as binding sites for the Cbx2/M33 chromodomain, thereby recruiting the PRC1 complex. Thus, the 2 PcG complexes could function in a cooperative manner to maintain gene silencing [1]. Among the PRC1 components, Bmi1 and Phc1 have been implicated in hematopoietic stem cell (HSC) self-renewal [2-5], a process by which epigenetic cellular memory is precisely inherited by daughter cells. We previously reported that Bmi1 plays a central role in the maintenance of self-renewing HSCs, whereas Cbx2 is dispensable in this process [3]. On the other hand, Cbx2 is essential for lymphopoiesis, as are the other PRC1 components, including Bmi1 and Phc1 [5,6]. Analysis of the tissue expression of human PcG proteins has demonstrated that PcG protein expression varies among tissues and even among specific cell types within a particular tissue, indicating that the composition of PcG complexes varies in tissue- and cell type–specific manners [7]. The compositions of PRC complexes, which have been characterized in *Drosophila* and mammalian cell lines, determine target and/or substrate specificities [8-10]; however, little is known about these complexes in primary hematopoietic cells, particularly in HSCs because of the limited numbers of these cells.

Our detailed reverse transcriptase–polymerase chain reaction analysis of mouse hematopoietic cells revealed that the genes for all of the PRC1 components that we analyzed, including *Cbx2*, *Phc1*, *Bmi1*, and *Rnf110*, are highly expressed in $CD34^-KSL$ HSCs, which make up only 0.004% of bone marrow mononuclear cells [11], and that sustained expression is evident in lymphoid-lineage cells [3]. To understand the differentiation stage–specific functions of PRC1, we used immunocytochemical staining and examination with a confocal microscope to analyze the subcellular localization of PRC1 components in purified $CD34^-KSL$ HSCs, $CD34^+KSL$ multipotential progenitor cells (MPPs), Lin^- progenitor cells, $B220^+CD43^+$ pro–B-cells in bone marrow, and $CD4^-CD8^-$ double-negative T-cells in thymus, as we have previously described [12]. The PRC1 components were primarily distributed in the euchromatic region of the nucleus, and Cbx2 and Bmi1 or Phc1 (Figures 1A and 1B), Cbx2 and Rnf110 or Scmh1 (data not shown), Ring1b and Bmi1 or Phc1 (Figures 1C and 1D), and Ring1b and Rnf110 or Scmh1 (data not shown) largely colocalized with one another in all cells analyzed, except for $CD34^-KSL$ HSCs

Correspondence and reprint requests: Atsushi Iwama, 1-8-1 Inohana, Chuo-ku, Chiba, Japan: 81-43-226-2187; fax: 81-43-226-2191 (e-mail: aiwama@faculty.chiba-u.jp).

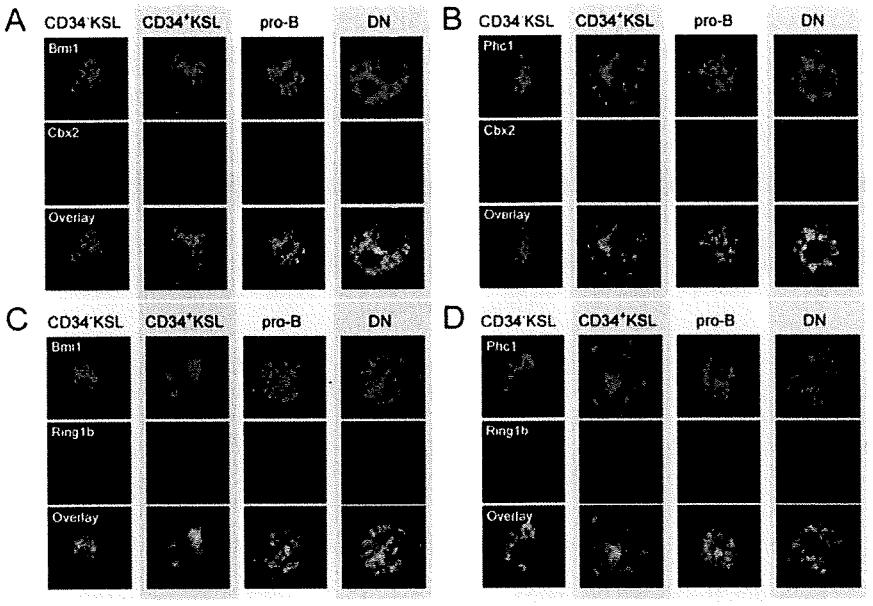

Figure 1. Hematopoietic stem cell (HSC)-specific polycomb repressive complex 1 (PRC1) with a unique composition devoid of Cbx2. $CD34^-KSL$ HSCs, $CD34^+KSL$ multipotential progenitor cells, pro–B-cells (pro-B) ($B220^-CD43^+$) in bone marrow, and double-negative (DN) ($CD4^-CD8^-$) T-cells in thymus were immunostained for Bmi1 (green) and Cbx2 (red) (A), Phc1 (green) and Cbx2 (red) (B), Bmi1 (green) and Ring1b (red) (C), and Phc1 (green) and Ring1b (red) (D). Nuclei were visualized by 4,6-diamidino-2-phenylindole (DAPI) staining (blue). The antibodies used and their manufacturers are as follows: mouse anti-Bmi1 monoclonal antibody (229F6; Upstate Biotechnology, Lake Placid, NY, USA); mouse anti-Phc1, anti-Rnf110, and anti-Scmh1 monoclonal antibodies (provided by H.K.); rabbit anti-Cbx2 and anti-Ring1b polyclonal antibodies (provided by M.V.); and Alexa Fluor 488 goat antimouse immunoglobulin G (IgG) and Alexa Fluor 647 goat antirabbit IgG secondary antibodies (Molecular Probes, Eugene, OR, USA). Immunofluorescence was observed with a Leica TCS SP2 AOBS confocal microscope (Leica, Wezlar, Germany).

(Lin^- progenitor cell data are not shown). This finding indicates that these components are constantly included in PRC1 throughout the process of hematopoietic differentiation from MPPs to lymphocytes, although the stoichiometry of each component could vary with the target gene loci and the differentiation stages. Notably, however, Cbx2 was largely excluded from PRC1, specifically in $CD34^-KSL$ HSCs. In most $CD34^-KSL$ HSCs analyzed (93.3%, n = 30), the vast majority of Cbx2 protein was located in the peripheral euchromatic region in discrete dots, whereas the other

Table 1.
Subcellular Colocalization and Functions of Polycomb Repressive Complex 1 (PRC1) Components in Hematopoietic Cells*

	Colocalization with Other PRC1 Proteins (Present Study)				Defects in Knock-out Mice [2-6]	
PRC1 Proteins	HSC	MPP	pro-B	DN	HSC	Lymphopoiesis
Cbx2/M33 (Cbx4/Mpc2)	–	+	+	+	No	Yes
Phc1/Mph1/Rae28 (Phc2/Mph2)	+	+	+	+	2+	Yes
Bmi1	+	+	+	+	3+	Yes
Rnf110/Mel-18 (Ring1/Ring1a)	+	+	+	+	1+	Yes
Rnf2/Ring1b	+	+	+	+	†	†
Scmh1 (Scml2)	+	+	+	+	†	†

*Proteins in parentheses were not assessed in this study. HSC indicates hematopoietic stem cells; MPP, multipotential progenitor cells; pro-B, pro–B-cells; DN, double-negative $CD4^-CD8^-$ cells.
†Data not available from the literature.

PRC1 components, including Bmi1, Phc1 (Figures 1A and 1B), Rnf110, and Scmh1 (data not shown), were located in the central euchromatic region separately from Cbx2.

The subcellular colocalization results and recent findings from loss-of-function analyses of PRC1 components in the hematopoietic system are summarized in Table 1. The loss of Cbx2, Phc1, Bmi1, or Rnf110 similarly caused hypoplastic spleen and thymus because of defective lymphopoiesis [6]. On the other hand, we and others have demonstrated the differential contribution of PRC1 components to the maintenance of self-renewing HSCs. The loss of function of Bmi1 was preferentially linked with a profound defect in HSC self-renewal, and loss of function of Mph1 led to the same defect, but to a lesser extent [3,4]. In overexpression experiments, *Bmi1* induced a striking ex vivo expansion of multipotential progenitors and markedly augmented HSC repopulating capacity in vivo [3]. *Rnf110*, a polycomb gene that is highly related to *Bmi1* in domain structure, also showed mild but significant effects in both loss-of-function and gain-of-function analyses [3]. By contrast, *Cbx2*$^{-/-}$ fetal liver hematopoietic cells exhibited a normal repopulating capacity, and the forced expression of *Cbx2* unexpectedly induced an adverse effect on HSC self-renewal and caused accelerated differentiation into macrophages [3]. All these findings clearly point to a central role for Bmi1 in the maintenance of HSCs. The finding that Cbx2 is dispensable in the maintenance of HSCs is surprising. Both *Bmi1* and *Cbx2* are involved in the maintenance of the expression pattern of homeotic genes through development. In this process, strong dosage interactions between these 2 genes have been observed [13], and Cbx2 supposedly targets PRC1 to the locus with H3K27me3 epigenetically marked by PRC2. Our finding that Cbx2 is largely excluded from PRC1 in HSCs, but not in lymphocytes, provides a direct explanation for the dispensable role for Cbx2 in HSCs but its essential role in lymphopoiesis as one of the PRC1 components. We previously demonstrated that forced expression of *Bmi1* in CD34^{+}KSL MPPs had no effect on their colony-forming efficiency or did not confer a self-renewal capacity to them [3]. In this study, we clearly showed that HSCs and MPPs differ in their PRC1 compositions. Together with other proteins, Bmi1 forms a cell type–specific PRC1 complex and can exhibit different functions depending on the composition of the complex. The distinct complexes of different compositions exhibit differential histone substrate specificities [9,10]. The HSC-specific PRC1 complex is devoid of Cbx2 but might include another PcG family member, such as Cbx4. This unique composition may define the HSC-specific function of PRC1 in the establishment and maintenance of gene expression patterns essential for HSC self-renewal.

Acknowledgments

This work was supported in part by grants from the Ministry of Education, Culture, Sport, Science and Technology, Japan; Core Research for Evolutional Science and Technology (CREST) of Japan Science and Technology Corporation (JST); and the Japan Leukemia Research Fund. We thank Drs. Y. Tadokoro, S. Yamazaki, and N. Iwamori for their excellent technical assistance.

References

1. Sparmann A, van Lohuizen M. Polycomb silencers control cell fate, development and cancer. *Nat Rev Cancer*. 2006;6:846-856.
2. Park I-K, Qian D, Kiel M, et al. Bmi-1 is required for maintenance of adult self-renewing haematopoietic stem cells. *Nature*. 2003;423:302-305.
3. Iwama A, Oguro H, Negishi M, et al. Enhanced self-renewal of hematopoietic stem cells mediated by the polycomb gene product, Bmi-1. *Immunity*. 2004;21:843-851.
4. Ohta H, Sawada A, Kim JY, et al. Polycomb group gene *rae28* is required for sustaining activity of hematopoietic stem cells. *J Exp Med*. 2002;195:759-770.
5. Iwama A, Oguro H, Negishi M, Kato Y, Nakauchi H. Epigenetic regulation of hematopoietic stem cell self-renewal by polycomb group genes. *Int J Hematol*. 2005;81:294-300.
6. Raaphorst FM, Otte AP, Meijer CJ. Polycomb-group genes as regulators of mammalian lymphopoiesis. *Trends Immunol*. 2001;22:682-690.
7. Gunster MJ, Raaphorst FM, Hamer KM, et al. Differential expression of human Polycomb group proteins in various tissues and cell types. *J Cell Biochem*. 2001;81:129-143.
8. Strutt H, Paro R. The polycomb group protein complex of *Drosophila melanogaster* has different compositions at different target genes. *Mol Cell Biol*. 1997;17:6773-6783.
9. Kuzmichev A, Jenuwein T, Tempst P, Reinberg D. Different Ezh2-containing complexes target methylation of histone H1 or nucleosomal histone H3. *Mol Cell*. 2004;14:183-193.
10. Kuzmichev A, Margueron R, Vaquero A, et al. Composition and histone substrates of polycomb repressive group complexes change during cellular differentiation. *Proc Natl Acad Sci U S A*. 2005;102:1859-1864.
11. Osawa M, Hanada K-I, Hamada H, Nakauchi H. Long-term lymphohematopoietic reconstitution by a single CD34-low/negative hematopoietic stem cells. *Science*. 1996;273:242-245.
12. Yamazaki S, Iwama A, Takayanagi S-I, Etoh K, Ema H, Nakauchi H. Cytokine signals modulated via lipid rafts mimics niche signals and induce hibernation in hematopoietic stem cells. *EMBO J*. 2006;25:3515-3523.
13. Bel S, Core N, Djabali M, et al. Genetic interactions and dosage effects of polycomb group genes in mice. *Development*. 1998;125:3543-3551.

The EMBO Journal (2007) 26, 846–854 | © 2007 European Molecular Biology Organization | All Rights Reserved 0261-4189/07
www.embojournal.org

THE EMBO JOURNAL

Novel regulation of MHC class II function in B cells

Yohei Matsuki[1,9], Mari Ohmura-Hoshino[1,9], Eiji Goto[1], Masami Aoki[1], Mari Mito-Yoshida[1], Mika Uematsu[1], Takanori Hasegawa[2], Haruhiko Koseki[2], Osamu Ohara[3,4], Manabu Nakayama[4], Kiminori Toyooka[5], Ken Matsuoka[5,6], Hak Hotta[7], Akitsugu Yamamoto[8] and Satoshi Ishido[1,*]

[1]Laboratory for Infectious Immunity, RIKEN Research Center for Allergy and Immunology, Tsurumi-ku, Yokohama, Kanagawa, Japan, [2]Laboratory for Developmental Genetics, RIKEN Research Center for Allergy and Immunology, Tsurumi-ku, Yokohama, Kanagawa, Japan, [3]Laboratory for Immunogenomics, RIKEN Research Center for Allergy and Immunology, Tsurumi-ku, Yokohama, Kanagawa, Japan, [4]Kazusa DNA Research Institute, Kisarazu, Chiba, Japan, [5]RIKEN Plant Science Center, Tsurumi-ku, Yokohama, Kanagawa, Japan, [6]Laboratory of Plant Nutrition, Faculty of Agriculture, Kyushu University, Higashi-ku, Fukuoka, Japan, [7]Division of Microbiology, Department of Genome Sciences, Kobe University Graduate School of Medicine, Chuo-ku, Kobe, Hyogo, Japan and [8]Faculty of Bio-Science, Nagahama Institute of Bio-Science and Technology, Nagahama, Japan

The presence of post-translational regulation of MHC class II (MHC II) under physiological conditions has been demonstrated recently in dendritic cells (DCs) that potently function as antigen-presenting cells (APCs). Here, we report that MARCH-I, an E3 ubiquitin ligase, plays a pivotal role in the post-translational regulation of MHC II in B cells. MARCH-I expression was particularly high in B cells, and the forced expression of MARCH-I induced the ubiquitination of MHC II. In B cells from MARCH-I-deficient mice (MARCH-I KO), the half-life of surface MHC II was prolonged and the ubiquitinated form of MHC II completely disappeared. In addition, MARCH-I-deficient B cells highly expressed exogenous antigen-loaded MHC II on their surface and showed high ability to present exogenous antigens. These results suggest that the function of MHC II in B cells is regulated through ubiquitination by MARCH-I.

The EMBO Journal (2007) **26**, 846–854. doi:10.1038/sj.emboj.7601556; Published online 25 January 2007
Subject Categories: proteins; immunology
Keywords: antigen presentation; B cell; MHC class II; traffic; ubiquitination

Introduction

Ubiquitination is an essential post-translational modification of proteins that 'marks' proteins with ubiquitin molecules, often resulting in degradation (Hershko and Ciechanover, 1998). This modification is achieved through the action of three enzymes: ubiquitin-activating enzyme E1 (E1), ubiquitin-conjugating enzyme E2 (E2), and ubiquitin-protein ligase E3 (E3). E1 activates ubiquitin, and the activated ubiquitin is subsequently transferred to a substrate through the interaction of E2 and E3. Whereas E2 carries the activated ubiquitin, E3 conjugates ubiquitin moieties to the target substrate (Hershko and Ciechanover, 1998).

At present, ubiquitination is thought to play an important role in the degradation of membrane proteins through the induction of endocytosis (Dupre *et al*, 2004). In yeast, an E3, Rsp5p, has been reported to induce ubiquitination of the cytoplasmic tail of substrate proteins, a step that is necessary for the endocytosis and degradation of the substrate proteins (Dupre *et al*, 2004). Similarly, we and other groups have recently identified a novel family of E3 enzymes termed MIR family, whose catalytic domain is a variant RING domain (RINGv domain). The MIR family members have been shown to induce rapid endocytosis and degradation through the ubiquitination of the cytoplasmic tail of substrate proteins in mammals (Coscoy *et al*, 2001; Coscoy and Ganem, 2003; Goto *et al*, 2003; Bartee *et al*, 2004; Lehner *et al*, 2005; Ohmura-Hoshino *et al*, 2006a). The MIR family proteins share a secondary structure and the RINGv domain located at the amino terminus. They bind to the membrane through their hydrophobic domains located at the center, and possess two intracellular regions.

Most importantly, the forced expression of MIR family members was found to be capable of degrading immune recognition-related molecules, such as MHC class I (MHC I) and MHC II (Coscoy and Ganem, 2000, 2001; Ishido *et al*, 2000a, b; Fruh *et al*, 2002; Ohmura-Hoshino *et al*, 2006b). However, the physiological substrates for these novel ubiquitin ligases remain completely unknown. Among the MIR family members, c-MIR and MARCH-I are of particular interest, because they can efficiently degrade important proteins in the immune system, and the surface expression of MHC II has been shown recently to be regulated by ubiquitination in dendritic cells (DCs) that potently function as antigen-presenting cells (APCs) (Goto *et al*, 2003; Bartee *et al*, 2004; Ohmura-Hoshino *et al*, 2006b; Shin *et al*, 2006). Within the E3 catalytic domain and transmembrane regions, the amino-acid identity between c-MIR and MARCH-I is >80%, suggesting similar functions. As MARCH-I expression was reported to be restricted to secondary lymphoid tissues such as spleen and lymph node, we have been especially interested in the functional elucidation of MARCH-I (Bartee *et al*, 2004).

In this report, we demonstrate that in B cells, the surface expression of MHC II is regulated through ubiquitination by MARCH-I, and the ubiquitination does not contribute to the internalization of surface MHC II. In parallel with the stabilization of surface MHC II, we found that MARCH-I-deficient B cells highly expressed exogenous antigen-loaded MHC II on their surface and showed high ability to present exogenous antigens. Thus, our results suggest that the function of MHC

*Corresponding authors. Laboratory for Infectious Immunity, RIKEN Research Center for Allergy and Immunology, 1-7-22 Suehiro-cho, Tsurumi-ku, Yokohama, Kanagawa 230-0045, Japan.
Tel.: +81 45 503 7022; Fax: +81 45 503 7021;
E-mail: ishido@rcai.riken.jp
[9]These authors equally contributed to this work

Received: 21 August 2006; accepted: 20 December 2006; published online: 25 January 2007

II on the surface of B cells is regulated through ubiquitination by MARCH-I.

Results

MARCH-I is highly expressed in B cells

To identify MARCH-I mRNA *in vivo*, we first performed Northern blot analysis in various tissues. Consistent with a previous report (Bartee *et al*, 2004), MARCH-I mRNA expression was restricted to secondary lymphoid tissues, such as spleen and lymph node (Figure 1A). Next, we generated MARCH-I-specific antibodies (Abs) to identify MARCH-I protein. Initially, we were unable to detect MARCH-I protein by Western blot analysis in all the examined tissues. As the MARCH-I protein expression level was expected to be low, we performed immunoprecipitation (IP)–Western blot analysis. Also, in order to increase the S/N ratio for detection, matrix conjugated with 13F11D12 anti-MARCH-I monoclonal antibody (mAb) was employed for IP, and a biotin-conjugated 4526 anti-MARCH-I polyclonal Ab was used for Western blot analysis. The epitopes for mAb and polyclonal Ab are different, as described in 'Materials and methods.' As shown in Supplementary Figure 1C, we found a faint band (marked with *), whose MW is similar to that of a protein transcribed from the expected full-length MARCH-I cDNA. These results suggested that the MARCH-I protein expression levels are extremely low *in vivo*. To provide some clues to determine the physiological role of MARCH-I, we further examined the expression levels of MARCH-I mRNA in various hematopoietic cells in the spleen by real-time PCR. As shown in Figure 1B, MARCH-I mRNA was highly expressed in B cells, and among splenic B cells, follicular B cells in particular highly expressed MARCH-I mRNA (Figure 1C). DCs and macrophages moderately expressed MARCH-I mRNA, whereas the expression was relatively low in splenic T cells, suggesting that MARCH-I might mainly function in APCs.

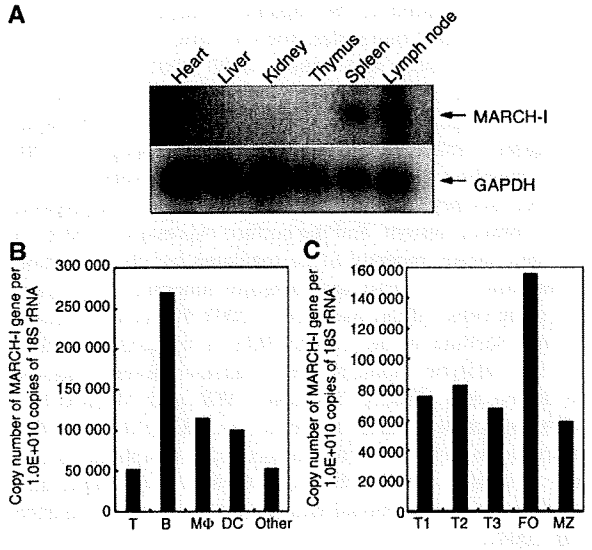

Figure 1 Expression profile of MARCH-I mRNA. (**A**) Expression profile of MARCH-I mRNA was analyzed by Northern blot in the indicated tissues. Data are representative of two independent experiments. (**B**) Expression levels of MARCH-I mRNA were compared among the indicated cell fractions in splenocytes. Data are representative of two independent experiments. (**C**) Expression levels of MARCH-I mRNA were compared among the indicated cell fractions in splenic B cells. Data are representative of two independent experiments. FO, follicular B cells; MZ, marginal zone B cells.

Downregulation and ubiquitination of MHC II by forced expression of MARCH-I

Next, we examined whether MARCH-I is functionally equivalent to c-MIR, using a 293T reconstitution system reported earlier (Ohmura-Hoshino *et al*, 2006b). As shown in Figure 2A, MARCH-I downregulated the surface expression of MHC II reconstituted with wild-type the I-A β chain. In contrast, the surface expression of MHC II reconstituted with the I-A β chain mutant, whose cytoplasmic lysine (the lysine residue at position 225 in the I-A β chain) was mutated to arginine, was not downregulated by MARCH-I. Also, a MARCH-I mutant, whose RINGv domain was disrupted by point mutation, was not able to downregulate MHC II surface expression. Consistent with these observations, MARCH-I ubiquitinated the cytoplasmic lysine residue within the I-A β chain, and its activity was dependent on the structure of the RINGv domain (Figure 2B). The downregulation of MHC II surface expression was also observed in two different murine B cell lines, A20 and M12 C3 cells (Griffith *et al*, 1988; Harding *et al*, 1995) (Figure 2C and D). Taken together, the forced expression of MARCH-I pointed to its broad functional homology with c-MIR.

MHC II expression is regulated through ubiquitination of the I-A β chain by MARCH-I

To examine whether MHC II is a physiological substrate for MARCH-I, we generated MARCH-I KO by gene targeting. As shown in Supplementary Figure 1A, exon 6 encoding the RINGv domain was flanked by two loxP sequences. After confirmation of insertion of three loxP sequences and a Neo cassette by Southern blot analysis, these mice were crossed with CAG-cre mice (Sakai and Miyazaki, 1997) to delete both exon 6 and the Neo cassette by cre-mediated recombination. Finally, two KO lines were established from two independent ES cells derived from 129 mice, as evaluated by Southern blot analysis (Supplementary Figure 1B). No MARCH-I protein was detected in these mice, demonstrating that these gene-targeted mice are indeed MARCH-I-null mice (Supplementary Figure 1C). FACS analysis did not show any significant abnormalities in the cellularity and development of T cells and B cells in the spleen (data not shown). Importantly, MHC II surface expression level was strikingly increased in the blood-circulating B cells from MARCH-I KO (Figure 3A). The extent of MHC II upregulation seems to parallel the extent of MARCH-I down-regulation. In contrast, the expression level of B7-1 was not altered (Figure 3A). Identical results were obtained from experiments with splenic B cells and splenic DCs in MARCH-I KO (data not shown). The same data were obtained from two different lines of MARCH-I KO.

To examine whether the amount of MHC II protein is increased in splenic B cells from MARCH-I KO, we analyzed the total amount of I-A β chain protein with 0.1% SDS-containing lysis buffer. As shown in Figure 3B, the amount of I-A β chain protein was significantly increased in splenic B cells from MARCH-I KO compared with control littermates. In contrast, as we expected, the expression level of I-A β chain

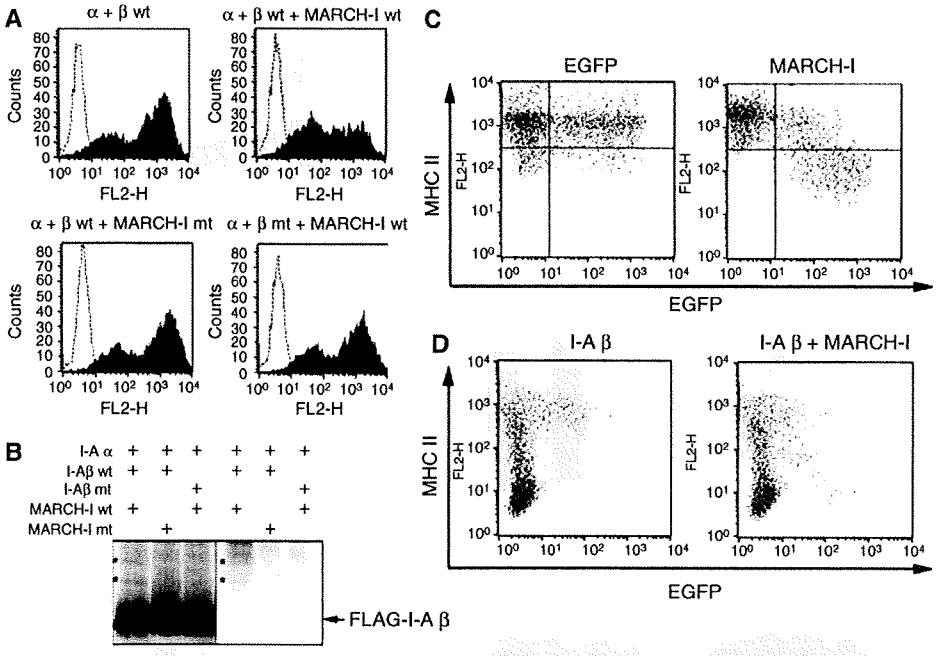

Figure 2 Downregulation and ubiquitination of MHC II by MARCH-I. (**A**) 293T cells were transfected with the expression plasmid indicated above each panel, with Fugene 6 reagent (Roche). Twenty-four hours after transfection, MHC II surface expression was analyzed by FACS. Data are representative of two independent experiments. (**B**) As indicated above each panel, 293T cells were cotransfected with several expression plasmids, and Flag-tagged I-A β chain was precipitated with anti-Flag Ab. Precipitated samples were probed with anti-Flag Ab (left) or anti-ubiquitin Ab (right). The band corresponding to the ubiquitinated I-A β chain is marked (*) as shown. Data are representative of two independent experiments. (**C**) A20 cells were transfected with plasmid expressing EGFP and MARCH-I from different promoters (right). In the left panel, only EGFP protein was expressed as control. MHC II surface expression level was examined by FACS. Data are representative of two independent experiments. (**D**) In M12 C3 cells that express the I-A α, but not I-A β, chain, I-A β chain alone (left) or MARCH-I plus I-A β chain (right) was expressed by electroporation with EGFP-coexpressing plasmid used in (C). MHC II surface expression was examined by FACS. Data are representative of two independent experiments.

mRNA was not significantly altered as judged by real-time PCR, suggesting that the upregulation of MHC II occurs at the post-transcriptional level. To confirm this, pulse–chase analysis was performed. B cells from MARCH-I KO or control littermates were pulse-labeled with [^{35}S]methionine and [^{35}S]cysteine and chased for indicated periods. At the end of the chase periods, pulse-labeled proteins were immunoprecipitated with Y-3P anti-I-A^{b} β chain mAb that preferentially recognizes mature αβ dimers (Brachet *et al*, 1997), and the precipitated samples were boiled before SDS–PAGE. At 1 h of chase, bands corresponding to the I-A β chain in both groups showed maximal and identical intensities, suggesting that both types of B cells synthesize the same amount of mature MHC II (αβ dimers). In contrast, at 6 and 9 h of chase, the amount of remaining MHC II was significantly increased in MARCH-I KO, compared with control littermates (Figure 3C). Thus, the I-A β chain of MHC II protein was stabilized in splenic B cells from MARCH-I KO.

The data from experiments with forced expression of MARCH-I and experiments with MARCH-I KO strongly suggested that MHC II is a physiological substrate for MARCH-I. To test this hypothesis, we examined the status of ubiquitination of the I-A β chain in splenocytes. In the splenocytes from control littermates, the polyubiquitinated I-A β chains were clearly detected, but the ubiquitinated I-A β chains completely disappeared in the splenocytes from MARCH-I KO, demonstrating that the I-A β chain of MHC II is indeed a physiological substrate for MARCH-I (Figure 3D).

Furthermore, to confirm that MHC II surface expression is regulated by ubiquitination of the I-A β chain, we expressed the I-A β chain wild type (I-A β wt) or the I-A β chain mutant type, whose K225 was mutated to arginine (I-A β K>R), in bone marrow (BM) cells by using retrovirus that coexpress human CD8 as a marker, and generated chimeric mice with these modified BM cells. We also generated control chimeric mice with BM cells infected with control retrovirus expressing human CD8 alone. Eight weeks after reconstitution, blood-circulating B cells expressing the same level of human CD8 were analyzed among the three groups. As K225 in the I-A β chain is responsible for the downregulation and ubiquitination of MHC II by forcibly expressed MARCH-I (Figure 2A and B), B cells generated from the I-A β K>R-expressing virus-infected BM cells are expected to highly express MHC II, compared with B cells generated from the I-A β wt-expressing virus-infected BM cells. As shown in Figure 3B and E, cells generated from the I-A β wt-expressing virus-infected BM cells (I-A β wt) highly expressed MHC II compared with B cells generated from control BM cells (Cont), and B cells generated from the I-A β K>R-expressing virus-infected BM cells (I-A β K>R) showed even higher expression of MHC II than B cells generated from the I-A β wt-expressing virus-infected BM cells. In contrast, MHC I expression levels were indistinguishable among these groups. These results strongly suggest that in B cells, MHC II surface expression is regulated by ubiquitination of the I-A β chain.

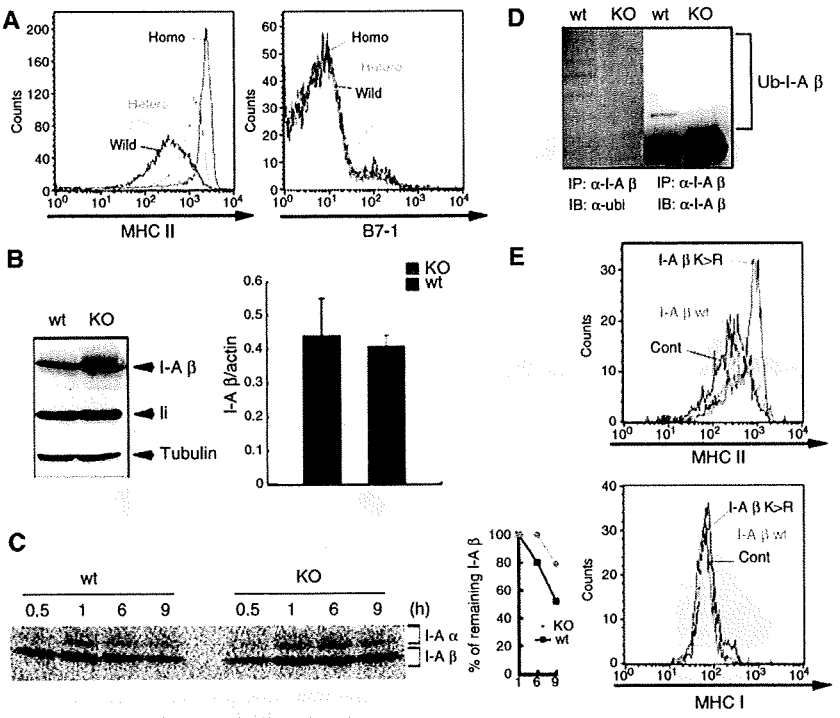

Figure 3 MHC II as a physiological substrate of MARCH-I. (**A**) MHC II (left) or B7-1 (right) surface expression was examined in blood-circulating B cells. Data from control littermates (wild), heterozygous MARCH-I KO (Hetero), and homozygous MARCH-I KO (Homo) are shown. Data are representative of two independent experiments. (**B**) In the left panel, I-A β chain protein or invariant chain (Ii) protein expression was examined in splenic B cells from respective mice. To show that the two samples have the same amount of loaded proteins, each sample was probed with anti-tubulin Ab. Data are representative of two independent experiments. Wt, control littermates; KO, homozygous MARCH-I KO. In the right panel, I-A β chain mRNA expression levels were compared between MARCH-I-deficient B cells (KO) and control B cells (Wt) by real-time PCR. Data are expressed as the mean ± s.d. of triplicate samples, and values are representative of two independent experiments. (**C**) Splenic B cells from each mouse were pulse-labeled with [^{35}S]methionine and [^{35}S]cysteine for 30 min and chased for 0.5–9 h. Labeled protein samples were extracted and precipitated with Y-3P anti-I-A β chain Ab and analyzed by SDS–PAGE. At each point, the percentage of remaining I-A β chain was calculated relative to the amount of labeled I-A β chain at 1 h of chase (right panel). Data are representative of three independent experiments. (**D**) MHC II molecules were purified with Y-3P anti-I-A β chain Ab, and subjected to Western blot analysis with FK2 anti-ubiquitin Ab (left) or KL295 anti-I-A β chain Ab (right). Data are representative of two independent experiments. (**E**) Sca-1$^+$ BM cells were infected with retrovirus that expresses the I-A β chain wild type (I-A β wt), I-A β chain mutant type (I-A β K > R), or human CD8 alone (Cont). Chimeric mice were generated with these modified BM cells. Eight weeks after reconstitution, blood-circulating B cells expressing the same level of human CD8 were analyzed in terms of MHC II expression level by FACS.

Surface MHC II molecules are stabilized in MARCH-I-deficient B cells

As shown in Figure 3A, MHC II surface expression was remarkably increased in B cells from MARCH-I KO. The next question was how the MHC II surface expression was enhanced in MARCH-I KO. MHC II surface expression level is regulated by several steps: the assembly between α and β chains, peptide loading onto αβ dimers, trafficking to the cell surface, and internalizing from the surface. As Figure 3C shows that the assembly of MHC II was not impaired in MARCH-I KO, we examined whether the formation of peptide-loaded αβ dimers was altered in MARCH-I KO. B cells from MARCH-I KO or control littermates were pulse-labeled as in Figure 3C. At the end of the chase periods, pulse-labeled proteins were immunoprecipitated with Y-3P anti-I-A^b β chain mAb, and the precipitated samples were analyzed by SDS–PAGE without boiling the samples before electrophoresis. As shown in Figure 4A, in both groups, bands corresponding to SDS-stable compact dimers, which reflect peptide-loaded αβ dimers (c(α/β)), were equally detected at 6 h of chase, suggesting that the step for peptide loading was not impaired.

Further, we examined whether the transport of MHC II to the surface was modified in MARCH-I KO. B cells from MARCH-I KO or control littermates were pulse-labeled as in Figure 4A, and at the end of the chase periods, the labeled cells were biotinylated with a membrane-impermeable reagent. The pulse-labeled and biotinylated MHC II molecules were immunoprecipitated with Y-3P mAb, followed by purification with streptavidin–agarose. As shown in Figure 4B, the transport efficiency of αβ dimers to the cell surface was slightly low in MARCH-I KO. Together, these findings did not explain how MHC II surface expression was increased in MARCH-I KO; rather, they suggest that the molecular events at the cell surface might be altered in MARCH-I KO. As the half-life of MHC II was prolonged (Figure 3C), we examined the half-life of surface MHC II in both types of mice. Surface MHC II molecules on splenic B cells were biotinylated and the stability of the biotinylated I-A β chains of MHC II was examined by IP–Western blot analysis. As MHC II surface expression was significantly upregulated in MARCH-I KO (Figure 5B), we used one-fifth of the total volume of each sample from MARCH-I KO at each chase point; otherwise,

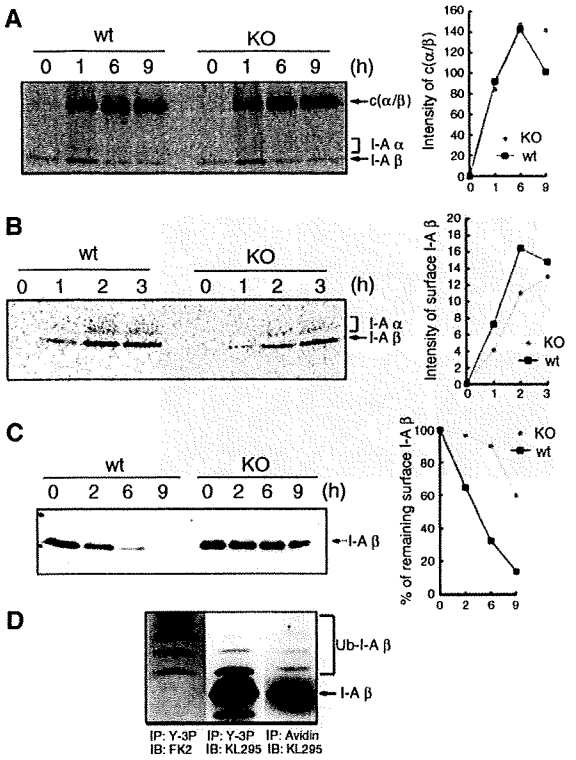

Figure 4 Stabilization of surface MHC II in MARCH-I-deficient B cells. (**A**) Splenic B cells from each mouse were pulse-labeled as shown in Figure 3C. Labeled protein samples were extracted and precipitated with Y-3P anti-I-A β chain Ab and analyzed by SDS–PAGE, without boiling the samples before electrophoresis. At each point, the intensity of SDS-stable compact dimer was measured with an image analyzer and presented far right from the panel. c(α/β) represents the SDS-stable compact dimer. Data are representative of two independent experiments. (**B**) Splenic B cells were pulse-labeled and chased as in (A). At the end of the chase periods indicated above the panel, each cell type was biotinylated with NHS-SS-biotin in PBS. The samples were precipitated with Y-3P anti-I-A β Ab, followed by precipitation with streptavidin–agarose. At each point, the intensity of the I-A β chain was measured with an image analyzer and presented far right from the panel. Data are representative of four independent experiments. (**C**) Surface MHC II molecules of splenic B cells were biotinylated and chased for 0–9 h. At each point, the amount of biotinylated MHC II was determined by Western blot analysis with KL295 anti-I-A β chain Ab, and the percentage of remaining surface I-A β was calculated relative to the value at 0 h (right panel). Data are representative of two independent experiments. (**D**) Surface MHC II molecules of splenic B cells from control littermates were biotinylated, purified with streptavidin–agarose, and analyzed with KL295 MHC II mAb (right panel). The same samples were incubated with Y-3P MHC II mAb and precipitated MHC II proteins were eluted with SDS buffer and analyzed with FK2 ubiquitin mAb (left panel) or KL295 MHC II mAb (middle panel). Data are representative of two independent experiments.

signals from the biotinylated I-A β chains from MARCH-I KO would have been too strong to enable precise comparison with those from control littermates. As shown in Figure 4C, the half-life of MHC II was significantly prolonged in B cells from MARCH-I KO. Collectively, these results indicate that MARCH-I modulates MHC II surface expression presumably through ubiquitination at the B cell surface. To investigate this hypothesis, we examined the status of ubiquitination of surface MHC II in B cells from control littermates. Surface MHC II molecules in B cells from control littermates were biotinylated, purified with streptavidin–agarose, and analyzed with KL295 MHC II mAb. The same samples were incubated with Y-3P MHC II mAb and precipitated MHC II proteins were analyzed with FK2 ubiquitin mAb or KL295 MHC II mAb. As shown in Figure 4D, in the sample purified with streptavidin–agarose, above the band corresponding to the unmodified I-A β chain, we detected additional bands showing similar MWs to those corresponding to the ubiquitinated I-A β chain. Thus, surface MHC II molecules in B cells were ubiquitinated.

MHC II molecules are internalized and recycled in MARCH-I-deficient B cells

We previously found that B7-2 was rapidly degraded in lysosome by c-MIR, suggesting that MHC II might be degraded in the same manner by MARCH-I (Goto *et al*, 2003). To investigate this possibility, the rate of degradation of surface MHC II was examined in the presence of bafilomycin A1, which raises endolysosomal pH through the inhibition of vacuolar H^+-ATPase. As shown in Figure 5A, the degradation of the surface I-A β chain was completely blocked in the presence of bafilomycin A1. Next, we examined whether the internalization of MHC II is inhibited in MARCH-I-deficient B cells, as we also found that surface MHC II molecules were rapidly internalized by c-MIR (Ohmura-Hoshino *et al*, 2006b). Surface MHC II molecules of MARCH-I-deficient B cells were biotinylated with a membrane-impermeable derivative of biotin. After incubation for 30 min, the remaining cell-surface biotin was cleaved with glutathione, and internalized proteins were collected using streptavidin-conjugated beads. The internalization rate of MHC II was analyzed with KL295 MHC II mAb. Unexpectedly, in MARCH-I KO, MHC II molecules were clearly internalized, as observed in control littermates (Figure 5B). These results demonstrate that ubiquitination is not essential for the internalization of MHC II in B cells.

These results suggest that ubiquitination mainly contributes to the sorting of MHC II into acidic organelles such as lysosome, for degradation, and in the absence of MARCH-I, internalized MHC II might be efficiently recycled to the surface, as MARCH-I-deficient B cells highly expressed MHC II on their surface (Figure 3A). To confirm these, we examined where the internalized MHC II molecules are localized in B cells from MARCH-I KO or control littermates. Surface MHC II molecules were labeled with FITC-conjugated AF6-120.1 anti-MHC II mAb at 4°C and chased for 60 min at 37°C. LysoTracker and transferrin were used to viably label the lysosomal compartment and the recycling compartment, respectively. To clearly visualize the internalized MHC II, labeled MHC II molecules remaining on the surface were removed with acidic solution. As shown in Figure 5C, MHC II molecules were internalized in both types of cells, and the amount of labeled MHC II detected inside MARCH-I-deficient B cells was larger than that detected inside B cells from control littermates. As expected, in B cells from control littermates, most internalized MHC II molecules were sorted into the lysosomal compartment (left panel in Figure 5C). In contrast, most internalized MHC II molecules were sorted into the recycling compartment in MARCH-I-deficient B cells (right panel in Figure 5C). Collectively, these results suggest

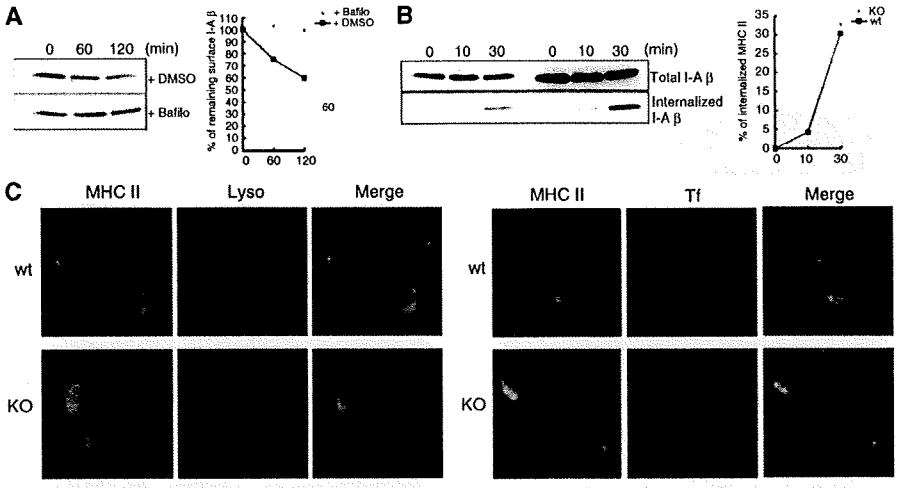

Figure 5 Internalization and recycling of MHC II in MARCH-I-deficient B cells. (**A**) Purified B cells were pretreated with 10 μM bafilomycin A1 (Bafilo) or DMSO at 37°C for 30 min. Surface MHC II molecules of pretreated cells were biotinylated and chased for 0–120 min. At each point, the amount of biotinylated MHC II was determined by Western blot analysis with KL295 anti-I-A β chain Ab, and the percentage of remaining surface I-A β chain was presented far right from the panel. Data are representative of two independent experiments. (**B**) Surface molecules of the same number of splenic B cells from MARCH-I KO or control littermates were biotinylated and incubated at 37°C for 10 or 30 min. At each point, the remaining cell-surface biotin was cleaved by reducing its disulfide linkage. Upper panel shows the total amount of biotinylated surface I-A β chains and lower panel shows the amount of internalized I-A β chains at each incubation time. At each point, the percentage of internalized MHC II was calculated relative to the total amount of biotinylated surface I-A β chains, and presented far right from the panel. Data are representative of four independent experiments. (**C**) Purified B cells were stained with FITC-conjugated AF6-120.1 anti-I-A β chain mAb at 4°C and washed with 2% calf serum-containing PBS. Labeled B cells were cultured in RPMI with 10% fetal calf serum in the presence of 50 nM LysoTracer Red DND-99 or 5 μg/ml Alexa 594-conjugated transferrin (Invitrogen) for 60 min at 37°C. Cells were washed in an acidic solution to remove uninternalized Abs, fixed, and subjected to examination with a LEICA DMIRE2 confocal laser scanning microscope.

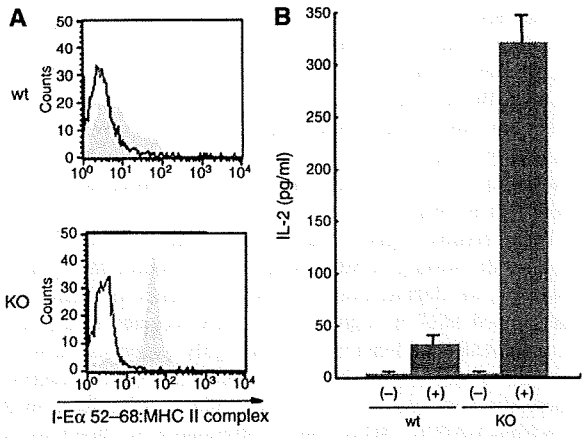

Figure 6 Enhanced antigen presentation by MARCH-I-deficient B cells. (**A**) Splenic B cells from each mouse type were incubated with 10 μM I-Eα peptide 52–68 for 20 h, and surface expression of I-Eα peptide-loaded MHC II was analyzed using Y-Ae mAb. Data are representative of two independent experiments. Open and shaded histograms show the values for non-incubation and incubation with peptide, respectively. (**B**) Splenic B cells incubated as in (A) were fixed with 0.5% paraformaldehyde and incubated with 20.6 T-T hybridoma overnight. IL-2 production from 20.6 T-T hybridoma was determined by enzyme-linked immunosorbent assay. Data are expressed as the mean ± s.e.m. of triplicate samples, and values are representative of two independent experiments. (–) and (+) indicate non-incubation and incubation with peptide, respectively.

that in B cells, MARCH-I-mediated ubiquitination of the I-A β chain leads to the sorting of MHC II into acidic organelles such as lysosome to regulate MHC II surface expression.

MARCH-I-deficient B cells highly present exogenous antigens through MHC II

As shown in Figure 3A, in MARCH-I-deficient B cells, the amount of surface MHC II was remarkably increased. The same result was obtained using Y-3P MHC II mAb that preferentially recognizes mature αβ dimers of MHC II, suggesting that surface MHC II expressed in MARCH-I-deficient B cells would be functional. To investigate this possibility, we examined whether MARCH-I-deficient B cells can express exogenous peptide-loaded MHC II on their surface. B cells from MARCH-I KO or control littermates were incubated with I-Eα peptide 52–68 for 20 h, and the surface expression of I-Eα peptide-loaded MHC II was monitored with Y-Ae mAb that specifically recognizes the complexes of I-A^b MHC II presenting the I-Eα peptide 52–68 (Rudensky *et al*, 1991). As shown in Figure 6A, MARCH-I-deficient B cells highly expressed I-Eα-peptide-loaded MHC II relative to B cells from control littermates. To confirm the enhanced presentation of the I-Eα peptide 52–68 in MARCH-I-deficient B cells, peptide-loaded B cells from MARCH-I KO or control littermates were fixed with 0.5% paraformaldehyde, and incubated with 20.6 T-T hybridoma that recognizes the MHC II–peptide complex detected with Y-Ae mAb (Ignatowicz *et al*, 1996). As shown in Figure 6B, IL-2 production from 20.6 T-T hybridoma was significantly enhanced in MARCH-I-deficient B cells. These results demonstrate that the expression of functional MHC II is increased in MARCH-I-deficient B cells.

Discussion

In this report, we demonstrated two important novel findings in B cells: the presence of post-translational regulation of

functional MHC II by ubiquitination, and the indispensable role of MARCH-I in MHC II ubiquitination. These important findings were based on the fact that the forced expression of MARCH-I downregulated MHC II surface expression through ubiquitination of the lysine residue at position 225 in the I-A β chain, and that surface functional MHC II molecules were stabilized owing to complete loss of ubiquitination of the I-A β chain of MHC II in MARCH-I-deficient B cells. Given that MHC II molecules are indispensable for T-cell-mediated immunity (Cosgrove *et al*, 1991), these novel findings serve as clues to understand the molecular basis of immune regulation.

MARCH-I was also expressed moderately in DCs and macrophages (Figure 1B), suggesting that MHC II is also regulated by ubiquitination in other APCs. Indeed, we found that MHC II expression was also augmented on the surface of bone-marrow-derived DCs (BMDCs) and splenic DCs in MARCH-I KO (Supplementary Figure 2A). In addition, the amount of ubiquitinated MHC II was decreased in BMDCs from MARCH-I KO, compared with those from control littermates (Supplementary Figure 2B). Interestingly, we found that in MARCH-I-deficient BMDCs, ubiquitinated MHC II did not completely disappear, indicating that other E3s might play a role in the ubiquitination of MHC II in BMDCs (Supplementary Figure 2B). In relation to this, we previously showed that c-MIR was expressed in DCs. c-MIR is a homologue of MARCH-I and acts to effectively downregulate and ubiquitinate MHC II (Ohmura-Hoshino *et al*, 2006b). Therefore, in DCs, c-MIR and MARCH-I might work together in ubiquitinating MHC II. On the other hand, in B cells, the expression level of c-MIR was extremely low (Ohmura-Hoshino *et al*, 2006b); thus, MARCH-I is thought to be a unique E3 for MHC II in B cells.

What is the role of MHC II ubiquitination in B cells? We showed that ubiquitination is crucial for the turnover of functional MHC II at the surface of B cells. In the absence of MARCH-I, an E3 for MHC II, the turnover of mature surface MHC II was decreased. As the results of experiments with Y-Ae mAb and I-Eα-specific T cell hybridoma indicated that stabilized MHC II molecules are capable of presenting exogenous antigens, MHC II ubiquitination might prevent excessive antigen presentation. In this connection, an important observation has been reported recently (Kitamura *et al*, 2006), strongly suggesting that MHC II surface expression is regulated by zinc-requiring enzymes. The catalytic domain of MARCH-I is a variant type of RING domain that requires zinc to maintain its structure and function as E3. DCs treated with TPEN, a zinc-chelating reagent, highly expressed MHC II on the surface and highly presented peptide antigens. Thus, in TPEN-treated DCs, MARCH-I might be inactivated owing to zinc deficiency, leading to an increase in MHC II surface expression. It would be interesting to investigate the status of MHC II ubiquitination in TPEN-treated DCs.

In order to answer the question of the role of MHC II ubiquitination in B cells, the results from MARCH-I KO have to be carefully interpreted, because other molecules might be targeted by MARCH-I *in vivo*. For example, the interpretation of the results showing increased ability of antigen presentation by MARCH-I-deficient B cells should be done with caution. Indeed, the forced expression of MARCH-I has been reported to downregulate transferrin receptor, B7-2, and Fas (Bartee *et al*, 2004). Therefore, to answer the question raised above, we are going to generate MHC II knock-in mice in which mutant I-A β, whose lysine residue at position 225 was mutated to arginine, is expressed in APCs. As shown in Figure 2B, mutant MHC II was not ubiquitinated by MARCH-I, so that in this knock-in mouse, the ubiquitination-mediated regulation of MHC II is expected to be disrupted.

In our experiments, we found that MHC II ubiquitination was not necessary for the internalization of MHC II in B cells. Previously, we demonstrated that the forced expression of c-MIR induced the rapid internalization of MHC II using A20 cells (Ohmura-Hoshino *et al*, 2006b). As c-MIR and MARCH-I are thought to share the molecular machineries for the downregulation of MHC II, we expected that MARCH-I contributes to the initiation of MHC II internalization from the plasma membrane. Unlike primary B cells used in this study, A20 cells might have different features of MHC II traffic. Indeed, we could not observe the spontaneous internalization of MHC II in A20 cells (Ohmura-Hoshino *et al*, 2006b). Thus, ubiquitination might play an important role in MHC II internalization in the situation where spontaneous internalization does not take place, such as in A20 cells. However, in the situation where spontaneous internalization takes place, ubiquitination might be no longer necessary for internalization. Recently, the contribution of the AP2 clathrin adaptor complex to the rapid internalization of MHC II was reported (Dugast *et al*, 2005; McCormick *et al*, 2005). It would be interesting to examine whether the AP2 complex is involved in the spontaneous internalization of MHC II in primary B cells.

MARCH-I is highly expressed in B cells. Why do B cells need MARCH-I? What happens when MHC II molecules are highly expressed in B cells? As long as the development of B cells was examined on the basis of the expression level of surface markers by FACS analysis, striking abnormalities could not be observed and a more fine-grained analysis is in order. In primary B cells, the molecular machinery for MHC II trafficking remains largely unknown. Our findings suggest that in native B cells, surface MHC II molecules are replaced with newly synthesized molecules through the degradation of pre-existing molecules, as is the case in immature DCs (Villadangos *et al*, 2005). Is this 'MHC II metabolism by MARCH-I' necessary for B cell homeostasis? We are going to answer numerous open questions that are yet to be addressed.

Materials and methods

Molecular cloning

Murine MARCH-I cDNA was generated from total RNA of the spleen by RT–PCR. The gene-targeting vector was generated using murine BAC clones. Substitutions were generated into the cytoplasmic tail of the I-A β chain by PCR-based mutagenesis (Promega). To construct retroviral vectors, I-A β chain cDNA was subcloned into pMX-IRES-hCD8 (Yamasaki *et al*, 2006).

Mice

The *Xho*I-linearized gene-targeting vector was electroporated into R1 embryonic stem (ES) cells, and targeted ES cells were selected with G418. ES cell colonies were screened by Southern blot analysis. Four independent clones were injected into blast cysts and two independent clones gave rise to chimeric mice that transmitted the desired mutation to the germ line. Two independent gene-targeted mice were mated with CAG-Cre mice to generate MARCH-I KO. All mice were maintained under specific pathogen-

free conditions according to RIKEN's guidelines for animal facilities and used for analysis at 8–12 weeks of age.

Northern blot analysis and quantification by real-time RT–PCR
For Northern blot analysis, 2 μg of poly (A) + RNA was extracted from various tissues, transferred to Hybond-N + membrane (GE Healthcare Bio-Sciences), and probed with ^{32}P-labeled cDNA probes. For MARCH-I mRNA quantification, the TaqMan Gene Expression Assay (Applied Biosystems) was employed, as described previously (Ohmura-Hoshino *et al*, 2006b). Quantitative analysis of I-A β chain expression was performed as described previously (Goto *et al*, 2003).

Pulse–chase analysis
Cells were labeled in medium containing 50 μCi of [^{35}S]methionine and [^{35}S]cysteine (Perkin Elmer) for 30 min and chased for the indicated time. Labeled proteins were extracted with 1% NP 40 buffer (1% NP 40, 300 mM NaCl, and 50 mM Tris buffer (pH 7.4)) containing protease inhibitors, and incubated with Y-3P anti-I-A^b Ab. Precipitated labeled MHC II molecules were subjected to quantitative analysis using Fuji BAS 2500 (FUJIFILM Corporation).

Detection of the ubiquitinated I-A β chain
In order to detect ubiquitination of the exogenous I-A β chain, we employed a previous method (Ohmura-Hoshino *et al*, 2006b). For detection of endogenous MHC II ubiquitinated *in vivo*, cell lysate was obtained by extraction with 1% NP 40 buffer containing 5 mM ethylmaleimide, and MHC II molecules were precipitated with Y-3P anti-I-A^b Ab coupled with CNBr-activated Sepharose 4B (GE Healthcare Bio-Sciences). The precipitated MHC II molecules were eluted with 0.1 M glycine–HCl (pH 2.7). The eluted samples were subjected to Western blot analysis with KL295 anti-I-A β Ab (ATCC) or FK2 anti-ubiquitin Ab (AFFINITI).

Detection of MARCH-I protein
Two Abs to MARCH-I were generated. The 4526 polyclonal Ab was generated with a synthetic peptide, GCETKLKPLRKWEKLQMTTS, corresponding to amino acids 123–140 of MARCH-I. 13F11D12 mAb was generated with a synthetic peptide, GCLNMWKKSKISTMYYLNQD, corresponding to amino acids 18–35 of MARCH-I. Protein sample was extracted with 0.1% SDS–Tris buffer from the spleen, and MARCH-I protein was precipitated with 13F11D12 anti-MARCH-I Ab coupled with protein G Sepharose (GE Healthcare Bio-Sciences). The precipitated MARCH-I protein was eluted with 2% SDS-containing PBS, and the eluted samples were analyzed with biotinylated 4526 anti-MARCH-I Ab.

Immunofluorescence microscopy
Purified B cells were stained with FITC-conjugated AF6-120.1 anti-I-A β chain mAb (BD Immunocytometry System) at 4°C and washed with 2% calf serum-containing PBS. Labeled B cells were cultured in RPMI with 10% fetal calf serum (FCS) in the presence of LysoTracer Red DND-99 or Alexa 594-conjugated transferrin (Invitrogen) at 37°C. Cells were washed in an acidic solution to remove uninternalized Abs, fixed, and examined with a LEICA DMIRE2 confocal laser scanning microscope.

Analysis of stability of surface MHC II
Splenic B cells were incubated with Sulfo-NHS-biotin (2 mg/ml) (Pierce) in PBS for 2 min on ice and chased for the indicated times. At the end of the chase periods, the protein samples were extracted with 0.1% SDS-containing PBS, and biotinylated proteins were precipitated with streptavidin-agarose (Pierce). Precipitated biotinylated samples were analyzed with KL295 anti-I-A β chain Ab.

Bone marrow transfer
Sca-1$^+$ BM cells from C57BL/6 mice were purified with the MACS system (Miltenyi Biotec) and cultured at a density of 1×10^6 cells/ml in RPMI with 10% FCS, 10 ng/ml IL-7, and 100 ng/ml stem cell factor (PeproTech). At days 1 and 2, cells were infected with the I-A β-chain expressing retrovirus. Four days after infection, hCD8$^+$ cells were purified with the MACS system (Miltenyi Biotec) and transferred intravenously into irradiated (8.5 Gy) C57BL/6 mice. Eight weeks after transfer, examinations were performed.

Antigen presentation assay
Splenic B cells were incubated with 10 μM I-Eα peptide 52–68 for 20 h, and incubated B cells were stained with Y-Ae mAb that specifically recognizes the complexes of I-A^b MHC II presenting I-Eα peptide 52–68. Splenic B cells incubated with I-Eα peptides (3×10^5) were fixed with 0.5% paraformaldehyde for 10 min at room temperature, mixed with 20.6 T-T hybridoma (5×10^4) in 200 μl of a 96-well plate, and cultured overnight. IL-2 production from 20.6 T-T hybridoma was determined by enzyme-linked immunosorbent assay (BD).

Internalization assay
Internalization of MHC II was analyzed by cell-surface biotinylation assay. Splenic B cells were subjected to biotinylation on ice with the reversible membrane-impermeable derivative of biotin, sulfo-NHS-S-S-biotin (1.5 mg/ml) (Pierce), in PBS. Biotinylated B cells were incubated at 37°C for 30 min, and the remaining cell-surface biotin was cleaved by reducing its disulfide linkage with glutathione cleavage buffer. The internalized I-A β chain molecules were precipitated with streptavidin–agarose (Pierce) and analyzed with KL295 anti-I-A β chain Ab.

Cell preparation and reagents
Splenic B cells, T cells, macrophages, and DCs were purified from the spleens of C57BL/6 mice using the MACS system (Miltenyi Biotec). The fraction shown as 'other' indicates the cell fraction that contained no B cells, T cells, Mϕ or DCs. Among the splenic B cells, the T1, T2, T3, FO, and MZ fractions were collected based on the expression levels of B220, AA4.1. CD23 and were detected IgM using a FACS Vantage SE high-speed sorter (BD Immunocytometry System). HL3 CD11c Ab for DCs, 145-2C11 CD3 Ab for T cells, RA3-6B2 B220 Ab for B cells, and CI:A3-1 F4/80 for Mϕ were used for the MACS system. RA8-6B2 B220, AA4.1 C1qRp, R6-60.2 IgM, and B3B4 CD23 Abs were used for FACS Vantage. Immature DCs were prepared by culturing BM cells obtained from each mouse with GM-CSF (20 ng/ml) (Pepro Tech) for 7 days. Seven days after cultivation, immature DCs were purified using CD11c beads (Miltenyi Biotec).

Statistics
Data from enzyme-linked immunosorbent assay and real-time RT–PCR were analyzed with the Student's *t* test. Values with $P<0.05$ were considered significant.

Supplementary data
Supplementary data are available at *The EMBO Journal* Online (http://www.embojournal.org).

Acknowledgements

We thank T Hirano and T Kurosaki for encouragement and helpful discussion, K Inaba for providing Y-Ae mAb and 20.6 T-T hybridoma, M Kasai for providing Y-3P mAb, S Yamasaki for providing pMX-IRES-hCD8 and technical advice, A Furuno for technical advise, R Triendl for critical reading of the paper, and K Nakamura for paper preparation. This work was supported in part by a Grant-in-Aid for Scientific Research from the Ministry of Education, Science, Sports, and Culture (MEXT) of Japan and by the Japan Society for the Promotion of Science (JSPS).

References

Bartee E, Mansouri M, Hovey Nerenberg BT, Gouveia K, Fruh K (2004) Downregulation of major histocompatibility complex class I by human ubiquitin ligases related to viral immune evasion proteins. *J Virol* **78:** 1109–1120

Brachet V, Raposo G, Amigorena S, Mellman I (1997) Ii chain controls the transport of major histocompatibility complex class II molecules to and from lysosomes. *J Cell Biol* **137:** 51–65

Coscoy L, Ganem D (2000) Kaposi's sarcoma-associated herpesvirus encodes two proteins that block cell surface display of MHC class I chains by enhancing their endocytosis. *Proc Natl Acad Sci USA* **97:** 8051–8056

Coscoy L, Ganem D (2001) A viral protein that selectively downregulates ICAM-1 and B7-2 and modulates T cell costimulation. *J Clin Invest* **107:** 1599–1606

Coscoy L, Ganem D (2003) PHD domains and E3 ubiquitin ligases: viruses make the connection. *Trends Cell Biol* **13:** 7–12

Coscoy L, Sanchez DJ, Ganem D (2001) A novel class of herpesvirus-encoded membrane-bound E3 ubiquitin ligases regulates endocytosis of proteins involved in immune recognition. *J Cell Biol* **155:** 1265–1273

Cosgrove D, Gray D, Dierich A, Kaufman J, Lemeur M, Benoist C, Mathis D (1991) Mice lacking MHC class II molecules. *Cell* **66:** 1051–1066

Dugast M, Toussaint H, Dousset C, Benaroch P (2005) AP2 clathrin adaptor complex, but not AP1, controls the access of the major histocompatibility complex (MHC) class II to endosomes. *J Biol Chem* **280:** 19656–19664

Dupre S, Urban-Grimal D, Haguenauer-Tsapis R (2004) Ubiquitin and endocytic internalization in yeast and animal cells. *Biochim Biophys Acta* **1695:** 89–111

Fruh K, Bartee E, Gouveia K, Mansouri M (2002) Immune evasion by a novel family of viral PHD/LAP-finger proteins of gamma-2 herpesviruses and poxviruses. *Virus Res* **88:** 55–69

Goto E, Ishido S, Sato Y, Ohgimoto S, Ohgimoto K, Nagano-Fujii M, Hotta H (2003) c-MIR, a human E3 ubiquitin ligase, is a functional homolog of herpesvirus proteins MIR1 and MIR2 and has similar activity. *J Biol Chem* **278:** 14657–14668

Griffith IJ, Nabavi N, Ghogawala Z, Chase CG, Rodriguez M, McKean DJ, Glimcher LH (1988) Structural mutation affecting intracellular transport and cell surface expression of murine class II molecules. *J Exp Med* **167:** 541–555

Harding CV, France J, Song R, Farah JM, Chatterjee S, Iqbal M, Siman R (1995) Novel dipeptide aldehydes are proteasome inhibitors and block the MHC-I antigen-processing pathway. *J Immunol* **155:** 1767–1775

Hershko A, Ciechanover A (1998) The ubiquitin system. *Annu Rev Biochem* **67:** 425–479

Ignatowicz L, Kappler J, Marrack P (1996) The repertoire of T cells shaped by a single MHC/peptide ligand. *Cell* **84:** 521–529

Ishido S, Choi JK, Lee BS, Wang C, DeMaria M, Johnson RP, Cohen GB, Jung JU (2000a) Inhibition of natural killer cell-mediated cytotoxicity by Kaposi's sarcoma-associated herpesvirus K5 protein. *Immunity* **13:** 365–374

Ishido S, Wang C, Lee BS, Cohen GB, Jung JU (2000b) Downregulation of major histocompatibility complex class I molecules by Kaposi's sarcoma-associated herpesvirus K3 and K5 proteins. *J Virol* **74:** 5300–5309

Kitamura H, Morikawa H, Kamon H, Iguchi M, Hojyo S, Fukada T, Yamashita S, Kaisho T, Akira S, Murakami M, Hirano T (2006) Toll-like receptor-mediated regulation of zinc homeostasis influences dendritic cell function. *Nat Immunol* **7:** 971–977

Lehner PJ, Hoer S, Dodd R, Duncan LM (2005) Downregulation of cell surface receptors by the K3 family of viral and cellular ubiquitin E3 ligases. *Immunol Rev* **207:** 112–125

McCormick PJ, Martina JA, Bonifacino JS (2005) Involvement of clathrin and AP-2 in the trafficking of MHC class II molecules to antigen-processing compartments. *Proc Natl Acad Sci USA* **102:** 7910–7915

Ohmura-Hoshino M, Goto E, Matsuki Y, Aoki M, Mito M, Uematsu M, Hotta H, Ishido S (2006a) A novel family of membrane-bound e3 ubiquitin ligases. *J Biochem (Tokyo)* **140:** 147–154

Ohmura-Hoshino M, Matsuki Y, Aoki M, Goto E, Mito M, Uematsu M, Kakiuchi T, Hotta H, Ishido S (2006b) Inhibition of MHC class II expression and immune responses by c-MIR. *J Immunol* **177:** 341–354

Rudensky A, Rath S, Preston-Hurlburt P, Murphy DB, Janeway Jr CA (1991) On the complexity of self. *Nature* **353:** 660–662

Sakai K, Miyazaki J (1997) A transgenic mouse line that retains Cre recombinase activity in mature oocytes irrespective of the cre transgene transmission. *Biochem Biophys Res Commun* **237:** 318–324

Shin JS, Ebersold M, Pypaert M, Delamarre L, Hartley A, Mellman I (2006) Surface expression of MHC class II in dendritic cells is controlled by regulated ubiquitination. *Nature* **444:** 115–118

Villadangos JA, Schnorrer P, Wilson NS (2005) Control of MHC class II antigen presentation in dendritic cells: a balance between creative and destructive forces. *Immunol Rev* **207:** 191–205

Yamasaki S, Ishikawa E, Sakuma M, Ogata K, Sakata-Sogawa K, Hiroshima M, Wiest DL, Tokunaga M, Saito T (2006) Mechanistic basis of pre-T cell receptor-mediated autonomous signaling critical for thymocyte development. *Nat Immunol* **7:** 67–75

Molecular Cell

A Phosphorylated Form of Mel-18 Targets the Ring1B Histone H2A Ubiquitin Ligase to Chromatin

Sarah Elderkin,[1] Goedele N. Maertens,[3] Mitsuhiro Endoh,[4] Donna L. Mallery,[2] Nick Morrice,[5] Haruhiko Koseki,[4] Gordon Peters,[3] Neil Brockdorff,[1,6,*] and Kevin Hiom[2,6,*]

[1]Medical Research Council Clinical Sciences Centre, Faculty of Medicine, Imperial College London, Hammersmith Hospital Campus, Du Cane Road, London W12 ONN, UK

[2]Medical Research Council Laboratory of Molecular Biology, Hills Road, Cambridge CB2 2QH, UK

[3]Cancer Research UK, London Research Institute, 44 Lincolns Inn Fields, London WC2A 3PX, UK

[4]Department of Developmental Genetics, RIKEN Research Centre for Allergy and Immunology, RIKEN Yokohama Institute, 1-7-22 Suehiro, Tsutumi-Ku, Yokohama 230-0045, Japan

[5]MRC Protein Phosphorylation Unit, Sir James Black Centre, University of Dundee, Dundee DD1 5EH, Scotland, UK

[6]These authors contributed equally to this work.

*Correspondence: hiom@mrc-lmb.cam.ac.uk (K.H.), neil.brockdorff@csc.mrc.ac.uk (N.B.)

DOI 10.1016/j.molcel.2007.08.009

SUMMARY

Recent studies have shown that PRC1-like Polycomb repressor complexes monoubiquitylate chromatin on histone H2A at lysine residue 119. Here we have analyzed the function of the polycomb protein Mel-18. Using affinity-tagged human MEL-18, we identify a polycomb-like complex, melPRC1, containing the core PRC1 proteins, RING1/2, HPH2, and CBX8. We show that, in ES cells, melPRC1 can functionally substitute for other PRC1-like complexes in *Hox* gene repression. A reconstituted subcomplex containing only Ring1B and Mel-18 functions as an efficient ubiquitin E3 ligase. This complex ubiquitylates free histone substrates nonspecifically but is highly specific for histone H2A lysine 119 in the context of nucleosomes. Mutational analysis demonstrates that while Ring1B is required for E3 function, Mel-18 directs this activity to H2A lysine 119 in chromatin. Moreover, this substrate-targeting function of Mel-18 is dependent on its prior phosphorylation at multiple residues, providing a direct link between chromatin modification and cell signaling pathways.

INTRODUCTION

Polycomb group (PcG) repressor proteins were originally identified as factors involved in the maintenance of homeobox gene silencing during development in *D. melanogaster*. Further studies showed these factors to be conserved in a wide range of organisms, with key roles in developmental gene regulation, cell-cycle regulation, and pluripotency in embryonic stem (ES) cells (for recent reviews, see Jorgensen et al., 2006; Schwartz and Pirrotta, 2007).

Biochemical and genetic studies revealed that PcG proteins are components of at least two major multiprotein complexes, termed *p*olycomb *r*epressor complex 1 (PRC1) (Saurin et al., 2001; Shao et al., 1999) and PRC2 (Cao et al., 2002; Czermin et al., 2002; Kuzmichev et al., 2002; Muller et al., 2002). Other PcG complexes have also been described (Klymenko et al., 2006; Kuzmichev et al., 2004). Analyses of PRC1 in *D. melanogaster* (Shao et al., 1999), and subsequently in mammalian cells (Levine et al., 2002), defined the core components Polycomb (PC), posterior sex combs (PSC), polyhomeotic (PH), and RING1 (dRING). There are two or more homologs of each of these core proteins in human and other higher organisms. It remains to be determined whether these homologs have equivalent and/or unique functions.

Early studies demonstrated that purified and reconstituted PRC1 complexes can inhibit transcription and SWI/SNF-mediated chromatin remodeling (Francis et al., 2001; Shao et al., 1999). More recently, PRC1-like complexes, containing the core components RING1/2 and BMI1, were isolated from HeLa cells and shown to function as a ubiquitin E3 ligase that specifically monoubiquitylates histone H2A lysine 119, this activity being attributed to the RING2 (Ring1B) protein (Wang et al., 2004). Monoubiquitylated H2A (H2Aub1) is a relatively abundant histone modification, estimated to comprise 5%–15% of available nucleosomal H2A (West and Bonner, 1980). Genetic studies revealed that mouse cells deleted for Ring1B and the closely related homolog Ring1A, exhibit global loss of H2Aub1 (de Napoles et al., 2004).

Although the function of H2Aub1 remains to be determined, several pieces of evidence suggest that it is important for PRC1-mediated gene repression. First, PRC1 targets, such as *Hox* genes and the inactive X chromosome in mammals, are enriched for H2Aub1 (Cao et al., 2005;

de Napoles et al., 2004). Second, in *D. melanogaster*, a point mutation affecting only the RING finger domain of dRING results in a classical polycomb phenotype (Fritsch et al., 2003). Analysis of this mutant protein in vitro demonstrated concomitant loss of H2A E3 ubiquitin ligase activity (Wang et al., 2004).

While, in vitro, the histone ubiquitin ligase activity of mouse Ring1B can be stimulated by other subunits of PRC1 (Cao et al., 2005), subcomplexes containing either human RING1 (Ring1A) or RING2 (Ring1B) with BMI1 exhibited E3 activity equivalent to that of PRC1 purified from HeLa cells (Wei et al., 2006). Since addition of other PRC1 proteins to this latter subcomplex did not enhance its E3 activity, it is likely that the Ring1B/Bmi1 subcomplex comprises a minimal bipartite ubiquitin E3 ligase. Similar synergistic effects have been reported for the RING finger proteins Brca1 and Bard1, in which heterodimerization markedly stimulates the E3 ubiquitin ligase activity of Brca1 (Hashizume et al., 2001; Mallery et al., 2002). Furthermore, like Brca1/Bard1, the ubiquitin ligase function of Ring1B/Bmi1 is enhanced by autoubiquitylation (Ben-Saadon et al., 2006; Chen et al., 2002; Hashizume et al., 2001; Mallery et al., 2002).

Structural analysis of a Ring1B/Bmi1 complex (Buchwald et al., 2006; Li et al., 2006) revealed extensive interactions between the RING finger domains of Ring1B and Bmi1 and that the association with the ubiquitin-conjugating enzyme (E2) maps to a surface on Ring1B (Buchwald et al., 2006). Although Bmi1 is not required for E2 interaction, it has been shown to contribute to the stabilization of the PRC1 complex (Cao et al., 2005; Wei et al., 2006).

In mammals, there are at least four paralogs of the *D. melanogaster* RING finger protein PSC: Bmi1, Mel-18, MBLR, and NSPc1 (Akasaka et al., 2002; Brunk et al., 1991; van Lohuizen et al., 1991). Evidence suggests that these paralogs may interact with other PcG proteins to form a set of distinct but related complexes. Specifically, MBLR together with Ring1B is implicated in the E2F6 complex (Ogawa et al., 2002), and NSPc1 together with Ring1B and other PRC1 proteins is a component of a BCOR corepressor complex (Gearhart et al., 2006).

Mel-18 protein is 70% identical to Bmi1 at the amino acid level. Genetic experiments suggest that these proteins may have similar or overlapping functions. Mel-18 knockout mice exhibit homeotic transformations and cell-cycle deficiencies similar to those reported for Bmi1 mutants (Akasaka et al., 1996, 1997, 2001; van der Lugt et al., 1994), and the Mel-18 protein localizes to PRC1 target genes (Fujimura et al., 2006). Despite this, Mel-18 has not been identified in purified PRC1 or related complexes (Gearhart et al., 2006; Levine et al., 2002; Ogawa et al., 2002; Wang et al., 2004) and, unlike Bmi1, did not enhance the E3 ligase activity of Ring1B in vitro (Cao et al., 2005).

In this study, we investigated the function of this protein and whether it forms part of a functional polycomb repressive complex. We show that Mel-18 is indeed a component of a PRC1-like complex and that it can functionally substitute for Bmi1 in repressing *Hox* gene expression in ES cells. Furthermore, contrary to previous reports, we show that a holocomplex and a reconstituted Ring1B/Mel-18 subcomplex efficiently ubiquitylate H2A lysine 119. Interestingly, we find that a phosphorylated form of Mel-18 is important for targeting this complex to histone H2A lysine 119. Our results provide insights into the mechanism of action of H2A ubiquitin E3 ligase complexes and demonstrate a direct link between chromatin regulation by PcG repressor complexes and cell signaling pathways.

RESULTS

Affinity Purification of a Polycomb-like Complex

To investigate whether, like other polycomb proteins, MEL-18 is present in cells as part of a large multiprotein complex, we expressed and purified human MEL-18 protein, fused to a tandem affinity purification (TAP) tag, from 293T cells. Mass spectrometry analysis identified several proteins that copurify with MEL-18 (Figure 1A). These proteins, namely RING1/2, the short isoform of HPH2a (Yamaki et al., 2002; Tonkin et al., 2002), and CBX8, were previously identified as core PRC1 components (Shao et al., 1999; Levine et al., 2002). Other paralogs of HPH2 were present in substoichiometric amounts, suggesting that multiple MEL-18 complexes might exist in the cell. Importantly, the MEL-18 paralog BMI1 was not present in this complex, and, conversely, MEL-18 was not present in a PRC1-like complex isolated using TAP-tagged BMI1 (see Figure S1 in the Supplemental Data available with this article online). Thus, MEL-18 and BMI1 proteins are components of similar but mutually exclusive PRC1-like complexes. We subsequently refer to these complexes as MEL-18 PRC1 (melPRC1) and BMI1 PRC1 (bmiPRC1).

melPRC1 is also present in mouse ES cells. Nickel-affinity purification of Mel18-FlagHis expressed in BM3 ES cells, which lack endogenously expressed Mel-18 and Bmi1, also "pulled down" Ring1A, Ring1B, and mPh1, homologs of the human PRC1 proteins RING1/2 and HPH1 (Figures S2A and S2B). Copurification of mPh1, rather than mPh2, most likely reflects low levels of mPh2 expression in mouse ES cells (H.K. and M.E., unpublished data).

Regulation of *Hox* Gene Expression in Embryonic Stem Cells

Microarray-based gene expression profiles identified several *Hox* genes whose expression is upregulated in cells lacking Mel-18 and Bmi1 (H.K. and M.E., unpublished data). Using RT-PCR, we measured expression of several of these genes in independently derived clones of BM3 that overexpress Mel-18-FlagHis (BM3-1, BM3-2, and BM3-3). In these cells, expression of the *Hoxa1*, *Hoxa5*, *Hoxd4*, and *Hoxd8* genes was approximately 5- to 10-fold lower than in the parental BM3 cell line (Figure 1B). Downregulation of gene expression was not a general phenomenon, as expression

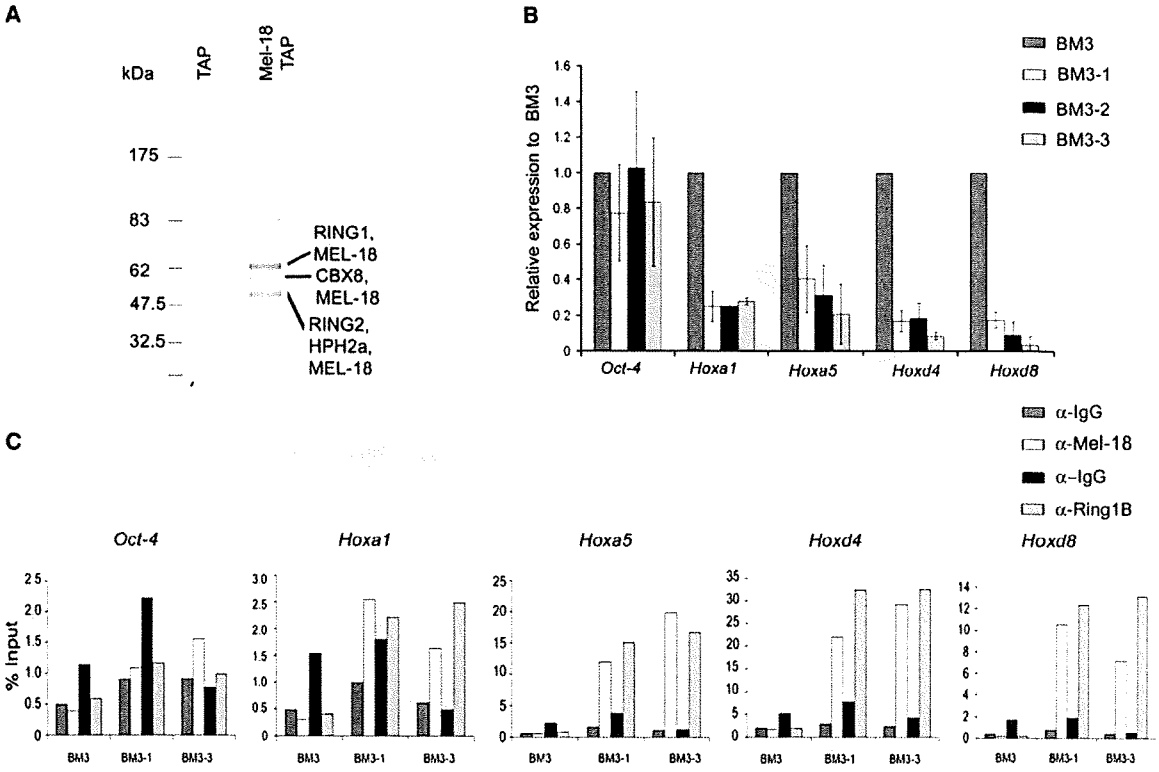

Figure 1. Mel-18 Forms a PRC1-like Complex that Represses *Hox* Gene Expression

(A) MEL-18 complex purified from 293T cells by TAP. Coomassie-stained gel showing proteins identified by mass spectrometry. Lane 1, proteins isolated by expression and purification of TAP alone, negative control. Lane 2, proteins isolated by expression and purification of TAP-Mel-18.

(B) Expression of *Hox* genes is downregulated in BM3 cells expressing Mel-18. Expression of *Hox* genes was analyzed by real-time RT-PCR in BM3 or BM3-1, BM3-2, and BM3-3, which express Mel-18-FlagHis. Gene expression levels were normalized against the average of two housekeeping genes (*GAPDH* and *HMBS*) and are represented as a ratio of expression in the parental cell line BM3. Expression of the *Oct-4*, *Hoxa1*, *Hoxa5*, *Hoxd4*, and *Hoxd8* genes is shown. Error bars represent the average standard deviation of five independent experiments.

(C) Mel-18 localizes to the promoter of *Hox* genes. ChIP was performed using antibodies against either Mel-18 or Ring1B at the promoter regions of *Oct-4*, *Hoxa1*, *Hoxa5*, *Hoxd4*, and *Hoxd8* in BM3-1 and BM3-3 cells. Antibody against IgG was used as a control. Enrichment is represented as a percentage of input. Replicate experiments are shown in Figure S3.

of the *Oct-4* gene in the same cells was unaffected by Mel-18. Therefore, like PRC1, melPRC1 may function as a negative regulator of *Hox* gene expression in ES cells.

Localization of melPRC1 to *Hox* Gene Promoters

To determine whether melPRC1 localizes to the promoters of *Hox* genes, we performed chromatin immunoprecipitation (ChIP) analysis. As expected, neither Mel-18 nor Ring1B was enriched at the promoters of *Hox* genes or *Oct-4* in parental BM3 cells (Figure 1C and Figure S3). However, in BM3-1 and BM3-3 cells, we observed enrichment of both Ring1B and Mel-18 at the promoters of *Hoxa1*, *Hoxa5*, *Hoxd4*, and *Hoxd8*, but not at *Oct-4* (Figure 1C and Figure S3). Hence, there is a clear correlation between the repression of gene expression and the recruitment of melPRC1 to the promoters of *Hoxa1*, *Hoxa5*, *Hoxd4*, and *Hoxd8*.

Ring1B/Mel-18 Complex Is a Ubiquitin E3 Ligase

Although Bmi1 and Ring1B interact to form a ubiquitin ligase complex that ubiquitylates nucleosomes in vitro, no such activity has been reported for Mel-18. We expressed and purified recombinant Mel-18 and Ring1B proteins in a complex, from Sf9 cells (Figures 2A and 2C). We noted that while Ring1B migrates as a single species, Mel-18 migrates as several distinct bands after polyacrylamide gel electrophoresis (Figure 2A). Subsequent analysis revealed these bands to be different phosphorylated forms of Mel-18 (see below).

Contrary to a previous report (Cao et al., 2005), we found that Ring1B/Mel-18, in the presence of the ubiquitin-conjugating enzyme (E2) UbcH5C, efficiently monoubiquitylates nucleosomes in vitro (Figure 2B). Like many other RING domain E3 ligases, Ring1B/Mel-18 also undergoes autopolyubiquitylation (Figure 2B), mainly on Ring1B (data not shown).

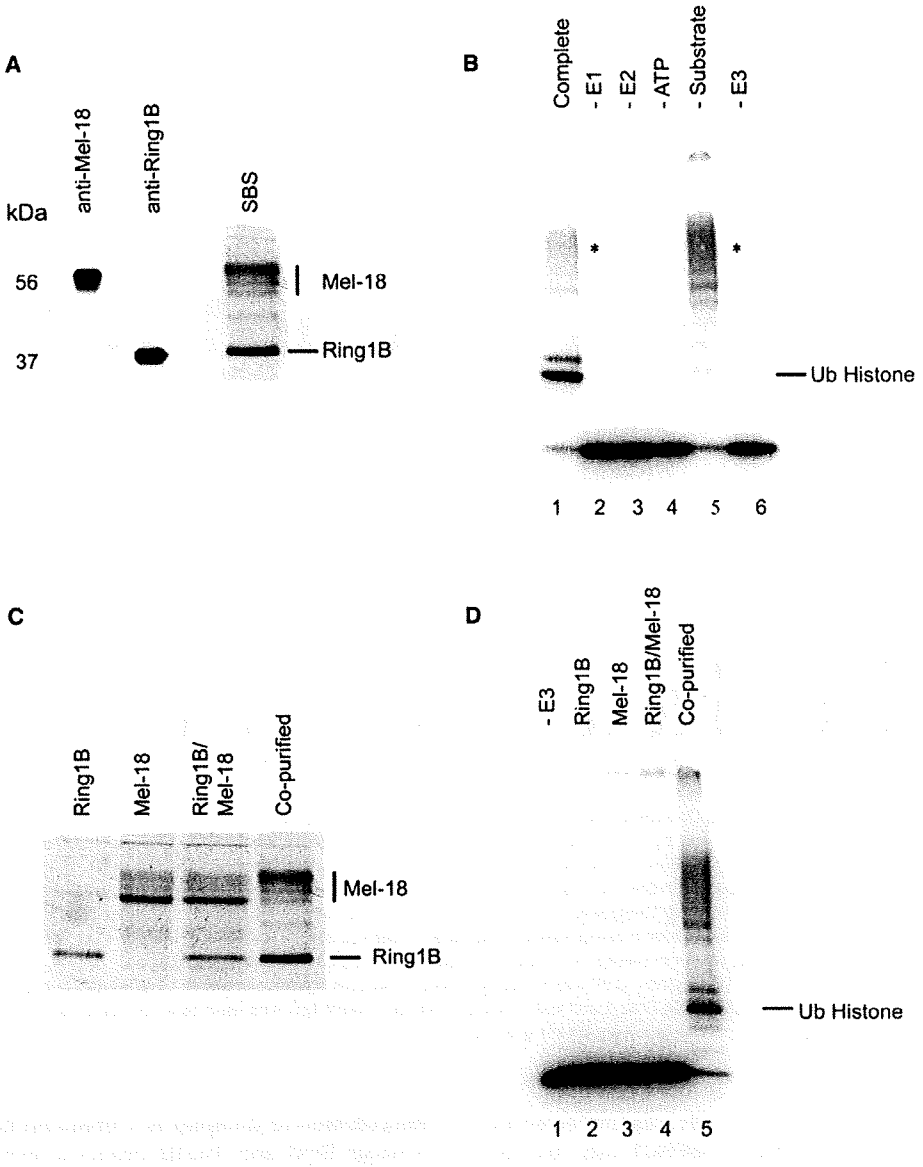

Figure 2. Ring1B/Mel-18 Complex Ubiquitylates Nucleosomes In Vitro

(A) FlagHis-tagged Ring1B and HA-tagged Mel-18 proteins were coexpressed and copurified from Sf9 cells as described in the Experimental Procedures. A 10 μl aliquot of the purified complex was analyzed by 12% SDS-PAGE and protein visualized by western blot using anti-Mel-18, anti-Ring1B antibodies (as indicated) or by staining with Simply Blue Safe Stain (Invitrogen) (SBS). Molecular weights are indicated.

(B) Ring1B/Mel-18-dependent ubiquitylation of chromatin requires ATP, E1, and E2 enzymes. Ubiquitylation assays were carried out as described in the Experimental Procedures with individual components omitted where indicated (lanes 2–6). The complete reaction is shown in lane 1. Ubiquitylated histone product is labeled. Autoubiquitylated Ring1B/Mel-18 complex is indicated by an asterix.

(C) Ring1B and Mel-18 were expressed and purified individually or as a complex from Sf9 cells. Proteins were visualized by staining with SBS. Shown are Ring1B alone (lane 1), Mel-18 alone (lane 2), Ring1B and Mel-18 mixed in vitro (lane 3), and copurified Ring1B/Mel-18 complex (lane 4).

(D) A complex of Mel-18 and Ring1B is required for efficient ubiquitylation of nucleosomes. Ubiquitylation assays were performed using the protein preparations described in the left panel.

We observed efficient ubiquitylation of nucleosomes only when Mel-18 and Ring1B were coexpressed and copurified as a complex (Figure 2D, lane 5). Neither Mel-18 or Ring1B purified individually nor a mixture of the two proteins exhibited strong E3 ligase activity (Figure 2D). This suggests, first, that both Mel-18 and Ring1B are required for the efficient ubiquitylation of nucleosomes and, second, that a factor (or factors)

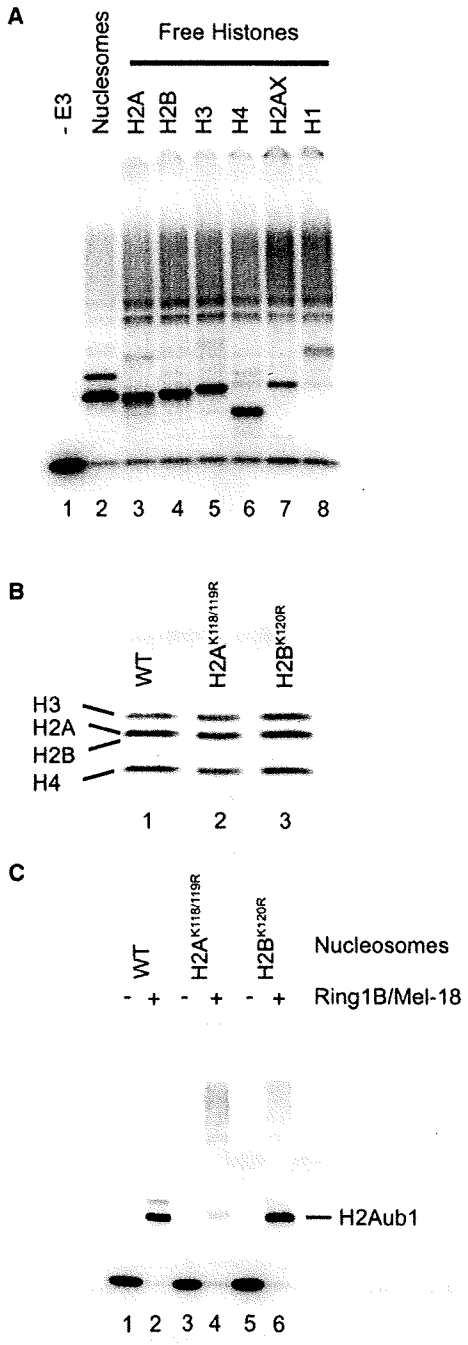

Figure 3. Ring1B/Mel-18 Complex Exhibits Defined Substrate Specificity

(A) Ubiquitylation assays were performed using 1 μg Ring1B/Mel-18 complex with various substrates, as indicated. Shown are 1.5 μg nucleosomes (lane 2); 1 μg of individual histones H2A, H2B, H3, and H4 (lanes 3–6); H2AX (lane 7); and H1 (lane 8). I^{125}-labeled products are shown.

(B) Purified reconstituted nucleosomes. Shown are wild-type nucleosome (lane 1), mutant $H2A^{K118/119R}$ nucleosome (lane 2), and mutant $H2B^{K120R}$ nucleosome (lane 3).

(C) Ubiquitylation of reconstituted nucleosomes by Ring1B/Mel-18 in vitro. Wild-type nucleosomes (lanes 1 and 2), histone $H2A^{K118/119R}$ mutant (lanes 3 and 4), and histone $H2B^{K120R}$ mutant (lanes 5 and 6) nucleosomes are shown.

present during the assembly of the Ring1B/Mel-18 complex in Sf9 cells plays an important role in activating the ubiquitin ligase function of the complex (see below).

Ring1B/Mel-18 Ubiquitylates Histone H2A

In vitro, Ring1B/Mel-18 seemed to ubiquitylate nucleosomes on a single histone (Figure 3A, lane 2). Modification was largely monoubiquitylation, although some diubiquitylated histone was also observed. We next investigated ubiquitylation of individual histones in vitro. We found that, whereas Ring1B/Mel-18 ubiquitylates individual nucleosome core histones with similar high efficiency, ubiquitylation of H1, the linker histone, was much less efficient (Figure 3A, lanes 3–8, respectively). Hence it appears that the Ring1B/Mel-18 complex acquires specificity for its histone substrate only in a nucleosomal context.

SDS-PAGE suggested that ubiquitylation of nucleosomes occurred on either histone H2A (H2Aub1) or histone H2B (H2Bub1). To investigate which of these histones is modified by Ring1B/Mel-18, we made nucleosomes with recombinant histone proteins in which either lysine 118 and 119 of H2A or lysine 120 of H2B were substituted with arginine residues (Figure 3B, lanes 2 and 3, respectively). We found that, whereas the Ring1B/Mel-18 ubiquitylated wild-type nucleosomes and those containing $H2B^{K120R}$ mutant with equal efficiency (Figure 3C, lanes 1 and 2 and 5 and 6, respectively), those made with $H2A^{K118/119R}$ were largely unmodified (Figure 3C, lanes 3 and 4).

Comparison of Mel-18/Ring1B with Bmi-1/Ring1B revealed that these complexes exhibit similar specific activity toward H2A on a nucleosomal substrate (Figure S4A). This was also the case when we compared the activity of melPRC1 and bmiPRC1 holocomplexes isolated from 293T cells (Figure S4B). We conclude that Ring1B/Mel-18 is a chromatin E3 ubiquitin ligase with specificity for lysines 118 or 119 of histone H2A. Again, this mirrors the specificity of the bmiPRC1 ubiquitin ligase and, because H2Aub1 is thought to be a repressive modification, is in keeping with the role of melPRC1 as a negative regulator of gene expression.

The Role of the Ring1B RING Domain in Ubiquitylation

RING domains are known to confer E3 ligase function. To investigate the role of the Ring1B RING domain in ubiquitylation of H2A, we made cysteine-to-glycine substitutions at residue 87 or 90, representing cysteines 7 and 8 of the RING domain (Figure 4A). We also made mutant protein with an isoleucine-to-alanine substitution at residue 53, which is critical for interactions with the

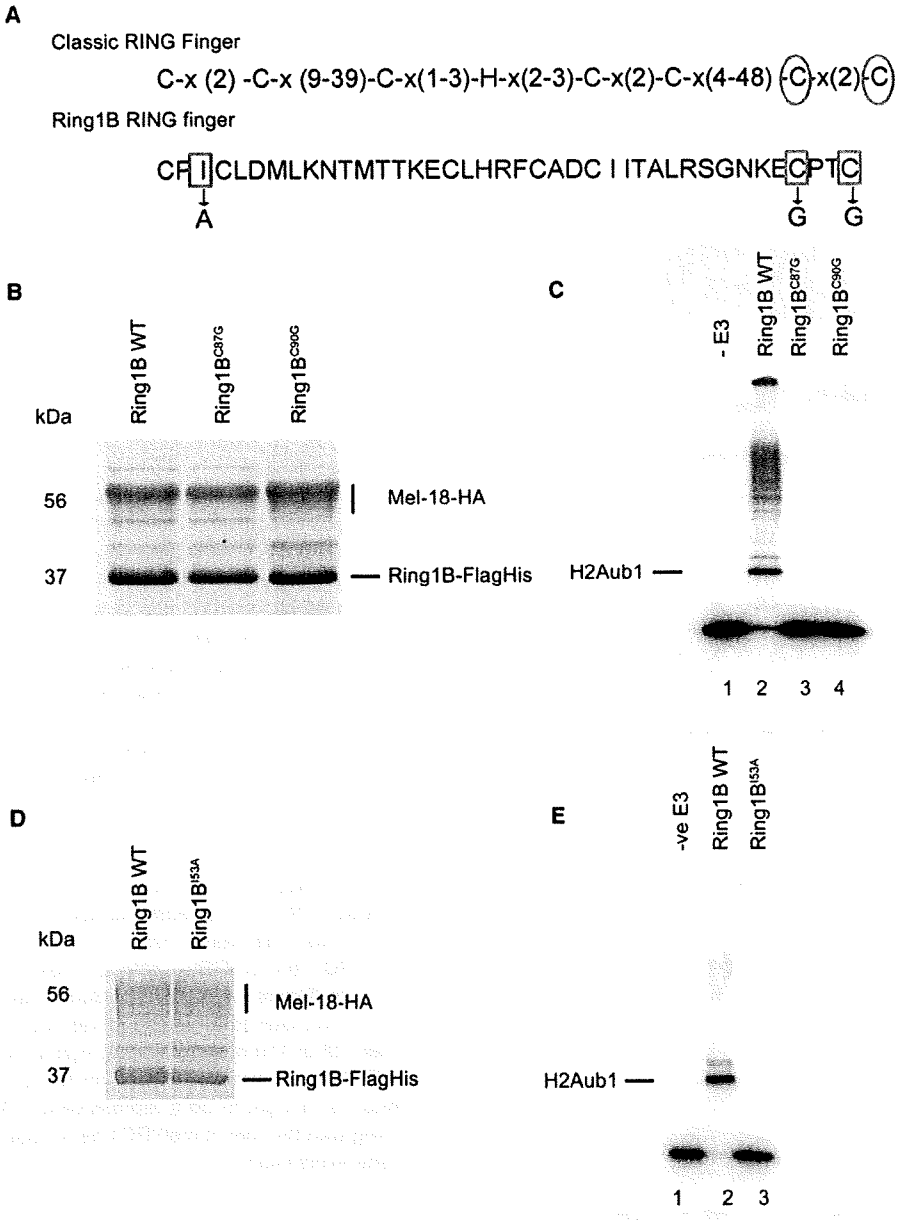

Figure 4. Mutations in the RING Domain of Ring1B Abolish the E3 Ligase Activity of the Ring1B/Mel-18 Complex

(A) Amino acid sequence of a consensus RING domain and the RING domain of Ring1B. Boxed residues represent the substituted amino acids and correspond to the circled residues of the consensus RING domain.

(B) Wild-type and mutant Ring1B/Mel-18 complexes. Wild-type, Ring1B^{C87G}/Mel-18, and Ring1B^{C90G}/Mel-18 complexes are shown. Molecular weight markers are indicated.

(C) Ring1B^{C87G}/Mel-18 and Ring1B^{C90G}/Mel-18 complexes were examined for E3 ligase activity in vitro. I^{125}-ubiquitylated histone H2A (H2Aub1) product is indicated.

(D) Wild-type and mutant Ring1B^{I53A}/Mel-18 complex.

(E) Mutant Ring1B^{I53A}/Mel-18 complex was examined for E3 ligase activity. Ubiquitylated H2A (H2Aub1) product is indicated.

ubiquitin-conjugating enzyme Ubc5C in other E3 ligases (Brzovic et al., 2003) (Figure 4A). Although these mutant proteins copurified normally with Mel-18 (Figures 4B and 4D), they were defective for the ubiquitylation of the nucleosome substrate and for autoubiquitylation (Figures 4C and 4E). In addition, these mutants were unable to ubiquitylate free histones (data not shown). We infer that the RING domain of Ring1B plays a central role in conferring